

Sensitivity of a Global Climate Model to the Specification of Convective Updraft and Downdraft Mass Fluxes

ANTHONY D. DEL GENIO

NASA/Goddard Space Flight Center, Institute for Space Studies, New York, New York

MAO-SUNG YAO

Sigma Data Services Corporation, NASA/Goddard Space Flight Center, Institute for Space Studies, New York, New York

(Manuscript received 1 December 1987, in final form 10 March 1988)

ABSTRACT

We examine the response of the GISS global climate model to different parameterizations of moist convective mass flux. A control run with arbitrarily specified updraft mass flux is compared to experiments that predict cumulus mass flux on the basis of low-level convergence, convergence plus surface evaporation, or convergence and evaporation modified by varying boundary layer height. An experiment that includes a simple parameterization of saturated convective-scale downdrafts is also described. Convergence effects on cumulus mass flux significantly improve the model's January climatology by increasing the frequency of occurrence of deep convection in the tropics and decreasing it at high latitudes, shifting the ITCZ from 12°N to 4°S, strengthening convective heating in the western Pacific, and increasing tropical long-wave eddy kinetic energy. Surface evaporation effects generally oppose the effects of convergence but are necessary to produce realistic continental convective heating and well-defined marine shallow cumulus regions. Varying boundary layer height (as prescribed by variations in lifting condensation level) has little effect on the model climatology. Downdrafts, however, reinforce many of the positive effects of convergence while also improving the model's vertical humidity profile and radiation balance. The diurnal cycle of precipitation over the West Pacific is best simulated when convergence determines cumulus mass flux, while surface flux effects are needed to reproduce diurnal variations in the continental ITCZ. In each experiment the model correctly simulates the observed correlation between deep convection strength and tropical sea surface temperature; the parameterization of cumulus mass flux has little effect on this relationship. The experiments have several implications for cloud effects on climate sensitivity. The dependence of cumulus mass flux on vertical motions, and the insensitivity of mean vertical motions to changes in forcing, suggests that the convective response to climate forcing may be weaker than that estimated in previous global climate model simulations that link convection only to moist static instability. This implies that changes in cloud cover and hence positive cloud feedback have been overestimated in these climate change experiments. Downdrafts may affect the feedback in the same sense by replenishing boundary layer moisture relative to cumulus parameterization schemes with only dry compensating subsidence.

1. Introduction

Cloud feedbacks are potentially among the most important contributors to climate sensitivity. Unfortunately, cloud processes are so poorly understood and crudely represented in climate models that even the sign of the total cloud feedback is in doubt. The most recent assessment by the National Academy of Sciences (Smagorinsky 1982) suggests that clouds are the principal cause of the large range of uncertainty in model estimates of climate sensitivity.

The parameterization of moist convection is a crucial element of any attempt to evaluate cloud feedbacks. Lindzen et al. (1982), for example, compared the re-

sponses to doubled CO₂ of a one-dimensional radiative-convective model with different representations of moist convection effects. They concluded that a simple penetrative convection scheme in which the updraft mass flux is proportional to surface heat and moisture fluxes gives a lower climate sensitivity than the traditional lapse-rate adjustment procedure because the cumulus scheme deposits heat at higher levels, from which it can be more effectively radiated to space. Their study used a clear sky radiative model, however, and thus did not incorporate any cloud/radiation feedbacks. Wang et al. (1981) considered cloud/convection feedbacks in a one-dimensional model with variable cloud height, optical thickness, and critical lapse rate. Their study illustrated the variety of feedbacks possible with interactive clouds and showed that the climate response could be different for different types of perturbations. Hansen et al. (1984) performed a doubled CO₂ experiment with interactive clouds in the GISS three-di-

Corresponding author address: Dr. Anthony D. Del Genio, NASA/GSFC, Institute for Space Studies, 2880 Broadway, New York, NY 10025.

mensional global climate model (GCM). They concluded that increased cloud height and decreased cloud cover due to stronger convection resulted in a significant positive cloud feedback.

Cumulus convection is also an important forcing mechanism for the general circulation through its release of latent heat and vertical transport of heat and momentum. As such, it is central to any proper simulation of the current climate and its low-frequency variability, especially in the tropics. Details of specifying the cumulus mass flux and heating profile have been shown to influence the Hadley circulation and ITCZ position (Yao and Stone 1987), the Walker circulation (Hartmann et al. 1984), and the 40–50 day oscillation (Chao 1987; Emanuel 1987; Lau and Peng 1987; Neelin et al. 1987). Convection effects on large-scale mid-latitude motions are secondary in comparison, but there is evidence, for example, that latent heat release alters the eddy forcing of the mean zonal wind and temperature (Stone and Salustri 1984).

Despite its obvious importance, cumulus parameterization in large-scale numerical models is still something of a primitive art. Processes such as momentum transport, entrainment, evaporation of condensate, and convective cloud formation are parameterized in ad hoc fashion in most models and completely neglected in some. Mesoscale organization, the importance of which has been documented in several field studies (Zipser 1977; Johnson 1984), has yet to be addressed in any GCM parameterization.

To this date, most of the research on cumulus parameterization has focused on the “closure assumption” of a scheme, i.e., its prediction of the instantaneous convective mass flux. Since convection can be viewed as an adjustment toward equilibrium of an atmospheric column destabilized by large-scale dynamic and radiative forcing, we can categorize all cumulus closures as belonging to one of two broad classes. One class attempts to relate cumulus mass flux directly to the nature of the forcing determined by other parts of the model. The forcing is usually specified in terms of the model’s large-scale convergence and the turbulent surface fluxes of moisture and heat. This approach is inherent in all CISK and evaporation–wind feedback models (cf. Lau and Shen 1988) as well as the more explicit cumulus parameterizations of Kuo (1965, 1974), Betts (1973), and Lindzen (1981).

Alternatively, one may calculate the mass flux needed to adjust the atmosphere to some specified state in one model time step. The adjustment may be toward an empirically determined constant lapse rate, a moist adiabat, or a state of constant convective instability. This philosophy is the basis for the moist convective adjustment method (Manabe et al. 1965) and the cumulus parameterizations of Arakawa and Schubert (1974) and Betts (1986).

It is difficult to assess the impact of existing schemes on the general circulation, hydrologic cycle, or climate

sensitivity of a GCM because of differences in other aspects of the GCMs in which they are used. A few limited comparisons of convection schemes within the same GCM have been published (cf. Baker et al. 1977; Miyakoda and Sirutis 1977; Donner et al. 1982; Geleyn et al. 1982; Hansen et al. 1983; Tiedtke 1984; Albrecht et al. 1986). However, a systematic evaluation of the physical processes underlying various closure assumptions is needed. In this paper we examine one aspect of schemes that parameterize the forcing explicitly by testing the effect of individual forcing terms for cumulus mass flux in the GISS GCM (Hansen et al. 1983). A separate set of experiments using an adjustment-type closure will be documented elsewhere. Some of our conclusions may, of course, be sensitive to the details of the particular convection scheme used in the GISS GCM. In fact, our experiments are strictly relevant only to parameterizations with an explicit cloud model. However, we feel that the differences among several of the experiments are sufficiently dramatic and straightforward to apply at least indirectly to the behavior of any GCM.

A related issue in penetrative-type cumulus parameterizations is the nature of the motions compensating the convective updraft. In existing schemes compensation takes place via large-scale gentle subsidence of the environment surrounding the clouds. This has the effect of warming and drying the lower atmosphere. In the past decade, though, it has become clear that convective-scale saturated downdrafts driven by precipitation loading and evaporation are important to the heat and moisture budgets of tropical cloud clusters (Johnson 1976; Zipser 1977; Knupp and Cotton 1985). Downdrafts can affect the vertical structure of a GCM because they cool the planetary boundary layer (PBL) and have higher humidity than the cloud-free environment, thus counteracting the effects of dry subsidence. This is potentially of interest for the cloud–climate feedback issue because it represents a qualitative change in the way convective events transport heat and moisture. We therefore also describe an experiment in which subsidence is partly replaced by a simple representation of saturated downdrafts.

In section 2 we briefly describe the basic model used and outline the series of experiments. The effects of the different mass flux parameterizations on the GCM’s convection patterns, thermodynamic and hydrologic state, general circulation, energy balance, and diurnal cycle are compared in section 3. We discuss the implications of our results for climate sensitivity, convection–SST relationships, and possible improvements in parameterization in section 4. Our concluding remarks are in section 5.

2. Model and experiment descriptions

The experiments were conducted with the most recent version of the GISS GCM (hereafter referred to as Model II), run at $8^\circ \times 10^\circ$ horizontal resolution

with nine vertical levels. A full description of the model and its climatology can be found in Hansen et al. (1983). Here we only briefly mention the important aspects of the GCM's moist convection parameterization. Model II uses a penetrative convection scheme with multiple cloud base levels and one cloud top level per instantaneous cloud base level. Convection is triggered if the moist static energy of a layer exceeds the saturation moist static energy of the layer above and the implied lifting produces saturation; this defines the cloud base. Fifty percent of the mass of the cloud base grid box rises in each event. The cloud top occurs at the top of the highest layer for which the cloud parcel is buoyant. Latent heat release serves only to maintain cloud buoyancy; heating/cooling of the environment takes place via compensating environmental subsidence, detrainment of cloud air at cloud top, and evaporation of falling condensate. Condensed water is not transported upward, but is allowed to reevaporate into 25% of each lower layer above cloud base and 50% below; the remainder determines the convective precipitation. The convective plume and subsiding environment transport grid-scale horizontal momentum. All types of convection are predicted by the same criteria; differentiation between deep and shallow depends only on the cloud buoyancy constraint.

In addition to the specification of cumulus mass flux, our experiments differ from the Model II formulation in several minor respects. 1) Convective cloud cover is set equal to the fraction of cloud base grid box mass that convects, as opposed to the Model II prescription of cloud cover proportional to the mean pressure thickness of all model layers up to cloud top. 2) A similar fraction of each grid box below cloud base, and half as much above, is available for condensate reevaporation instead of the constant 50%/25% used in Model II. 3) Plume condensate is computed using three iterations on the Clausius-Clapeyron equation rather than one. 4) Large-scale supersaturation clouds are computed every hour as opposed to every fifth hour in Model II.

For this study the GCM was run in a perpetual January mode with fixed climatological sea surface temperature (SST). Each experiment was run for four months; the diagnostics presented here represent averages over the last three months. Standard deviations for a five-year control run of the model are tabulated by Rind (1986); we restrict discussion to changes larger than several standard deviations whenever such information is available. We compare five experiments that differ only in the parameterization of convective mass flux:

1) *Control run.* This is essentially Model II except for the small changes noted above. Convective mass flux is specified arbitrarily to be one-half the mass of the cloud base grid box per physics time step whenever the instability criterion is satisfied.

2) *Mass flux based on convergence (Experiment W).* It is now well established that organized deep convection is favored by low-level convergence on larger scales (cf. Ogura et al. 1979; Thompson et al. 1979; Cooper et al. 1982; Graham and Barnett 1987). In this experiment we predict the cumulus mass flux M_c as

$$M_c = \rho_B w_B, \quad (1)$$

where ρ_B and w_B are the cloud base density and large-scale vertical velocity, respectively. When $w_B < 0$, convection does not occur even if the moist static instability criterion is satisfied. This parameterization encourages explicit CISK-type dynamical feedbacks, which can only occur indirectly, if at all, in Model II. Surface fluxes influence convection in this run only to the extent that they help produce unstable vertical profiles of moist static energy.

3) *Mass flux based on convergence plus surface flux (Experiment S).* Isolated deep convective events over land in summer are often tied to small-scale turbulence associated with surface heating (Byers and Braham 1949) rather than organized lifting. Likewise, shallow convection over oceans is at times driven by surface fluxes and often occurs in the presence of large-scale subsidence (cf. Holland and Rasmusson 1973; Agee and Dowell 1974; LeMone and Pennell 1976). Any parameterization used in a global model must be capable of producing these convective types. The surface flux contribution to the cumulus mass flux can be related to the rate at which turbulence deepens the PBL by entrainment (called the entrainment velocity, w_e). If cumulus subsidence is assumed to be just sufficient to balance the deepening due to large-scale lifting and PBL entrainment and keep PBL height (z_B) constant, we can write

$$M_c = \rho_B (w_B + w_e). \quad (2)$$

In mixed-layer models, w_e is calculated as the flux of heat or moisture through z_B divided by the discontinuity in that quantity at z_B . If sensible heat or virtual dry static energy is used, the unknown flux at z_B must be related to the surface flux via a poorly constrained scaling constant which represents the strength of frictional dissipation in the PBL. However, for an unsaturated mixed layer the flux of moisture is constant with height through the PBL when averaged over cloudy and cloud-free regions (Esbensen 1975; LeMone and Pennell 1976). Thus, since w_e can be expressed equivalently in terms of moisture or heat fluxes (Arakawa and Schubert 1974), we parameterize cumulus mass flux in this experiment as

$$M_c = \rho_B w_B + \frac{F_q}{\Delta q}, \quad (3)$$

where F_q is the surface evaporation and $\Delta q = q_+ - q_-$ is the jump in q across z_B . The GISS GCM does not calculate z_B explicitly, so we estimate it as the level top

below which potential temperature is constant to within 0.5 K. The value of q_- is then q at the highest such level and q_+ the interpolated value halfway between that level and the next highest. This assumption gives typical values of $\Delta q \approx 2-5 \text{ g kg}^{-1}$ over the tropical oceans, consistent with GATE observations (Nicholls and LeMone 1980). Equation (3) only applies when convection originates from a level below z_B ; when this is not true, Eq. (1) is used instead. Again, in all of the experiments, convection does not occur if either the instability criterion is not satisfied or the computed $M_c < 0$.

4) *Inclusion of varying PBL height (Experiment Z).* In general, PBL height can be expected to vary with time, for example, over land in afternoon when PBL deepening by entrainment can exceed suppression due to cumulus-induced subsidence. Equation (3) probably overstates the surface flux contribution to M_c in such cases. Arakawa and Schubert (1974) calculate M_c using the quasi-equilibrium assumption and use this to estimate the time rate of change of z_B following the flow. For our purposes an independent prediction of z_B is needed instead. Dry convection height may be useful as a climatological indicator of PBL height variations (cf. Hansen et al. 1983, Fig. 18), but GCM vertical resolution is too coarse to use it for instantaneous time derivatives. Albrecht (1983) suggests defining cloud base cumulus mass flux such that the top of the mixed layer is at the lifting condensation level z_{LCL} . The lifting condensation level (LCL) does in fact track changes in PBL height remarkably well in GATE composite easterly wave data (Johnson 1980, Fig. 16). Following Albrecht, we thus parameterize cumulus mass flux in this experiment as

$$M_c = \rho_B w_B + \frac{F_q}{\Delta q} - \rho_B \frac{\partial z_{LCL}}{\partial t}, \quad (4)$$

with the LCL calculated with respect to air at the lowest GCM level. Actually, Eq. (4) should also include horizontal advection of z_{LCL} ; in situations dominated by large moisture convergence, individual changes in LCL following the flow should be much smaller than the local changes we consider. Thus, Eq. (4) may overestimate the effect of PBL height variations on cumulus mass flux.

5) *Inclusion of convective downdrafts (Experiment D).* In this experiment we parameterize downdrafts for convective events that extend beyond one GCM level by testing as the plume rises for the first level (if any) at which an evaporatively cooled equal mixture of cloud and environmental air is negatively buoyant. If such a level is found, a downdraft forms there with the properties of the mixture. This is an oversimplification of the entrainment processes that produce downdrafts, but Betts (1982) has shown that for typical cumulus environments, roughly equal mixtures of cloud and environmental air are most likely to be neg-

atively buoyant. Furthermore, Johnson (1976) has shown that downdraft effects in a diagnostic model are insensitive to the exact specification of their thermodynamic properties at the level of origin. Once formed, the downdraft penetrates to cloud base (almost always the lowest GCM level), evaporating liquid water from levels below its level of origin as necessary to remain as close to saturation as possible. The updraft mass flux in this experiment is given by Eq. (4), and the downdraft mass flux is specified as a fixed percentage of the updraft mass flux, as suggested by the results of mesoscale numerical models (Simpson et al. 1982). We tested 25% and 50%, which span available estimates from field studies (Johnson 1976; Nitta 1978); the results presented here are for the latter case, which exhibits more dramatic effects. Dry environmental subsidence provides the remainder of the compensating mass flux. Above the downdraft formation level, M_c is reduced by the mass of cloud air incorporated into the downdraft.

The climatology of the control run is very similar to that of GISS Model II (see Figs. 20-44 in Hansen et al. 1983). Additional diagnostics relevant to the present discussion are shown in Figs. 1 and 2. Despite the simplicity of Model II's cumulus mass flux prescription, it produces a reasonable simulation of most aspects of the current climate compared to other GCMs. One deficiency of Model II is its tendency to produce peak precipitation at 12°N in January rather than slightly south of the equator as observed (Jaeger 1976). This result is correlated with the peak in moist convective mass flux, which also occurs at 12°N (Fig. 1a). Spurious midtroposphere local peaks in convection occur at high latitudes. The relative humidity profile (Fig. 1b) is qualitatively realistic, with a local maximum due to deep convection at the equator and minima at 20°N and 30°S in the subsiding branches of the Hadley cells. There is, however, too much water vapor in the upper troposphere and too little in the lower troposphere in the tropics compared to observations (Oort 1983). Tropical cloud cover (Fig. 1c) is regulated by convection, with large-scale cirrus tending to form at the level to which most tropical deep convection penetrates in the model (200 mb).

The geographical distribution of deep convective events (those which penetrate four or more model levels) traces the location of the model's ITCZ, SPCZ, and midlatitude cyclonic storm tracks (Fig. 2a). The GCM's undesirable maximum in precipitation at 12°N latitude is due to excessive convection in the Bay of Bengal, Indochina, and over the warm waters west of Central America. Deep convection typically occurs 10%-15% of the time in the most strongly convecting regions of the ITCZ; this is well below the 50%-80% frequency estimated for 8° × 10° areas in the ISCCP Pilot Data Set by Del Genio and Yao (1987). The discrepancy indicates that either the time-averaged cu-

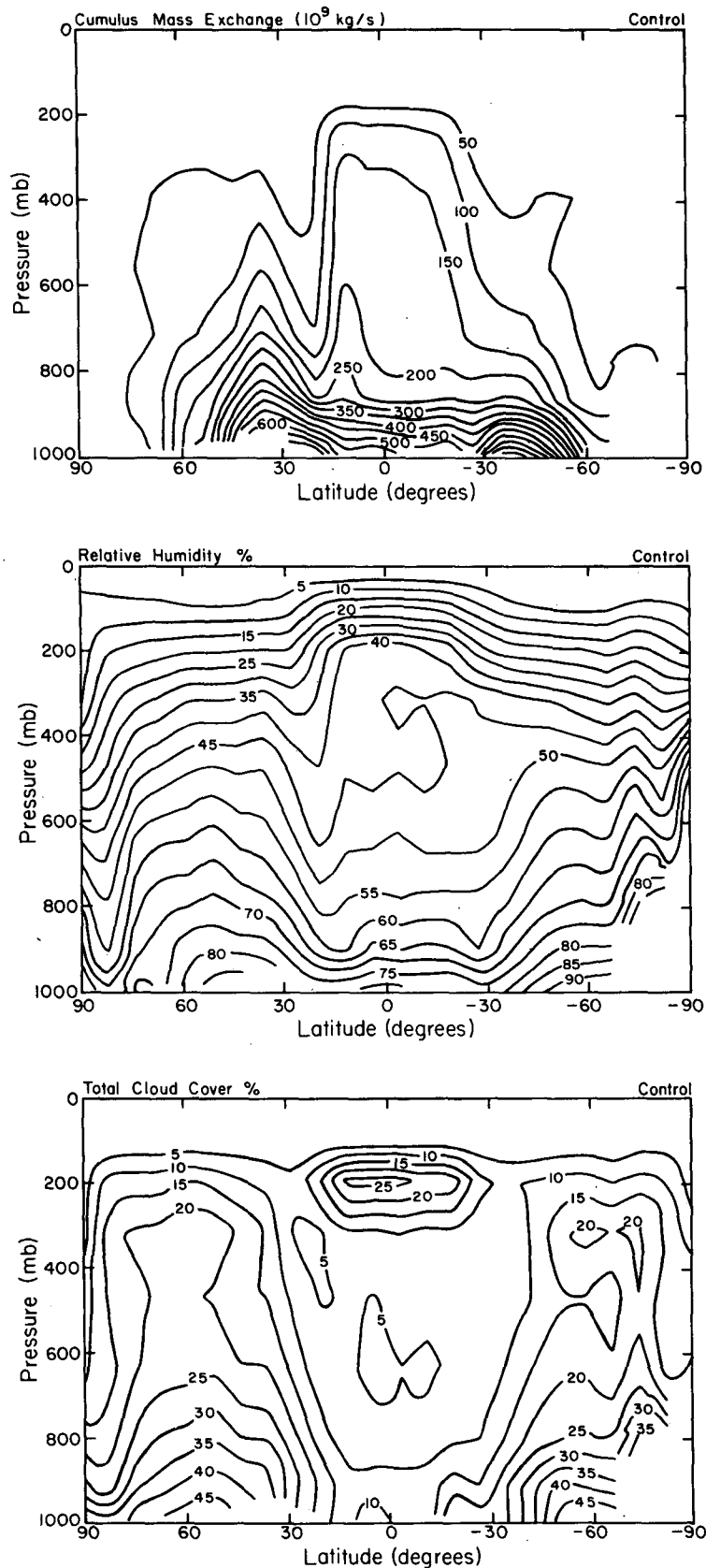


FIG. 1. Zonal mean distributions of cumulus mass exchange (upper), relative humidity (middle), and total cloud cover (lower) for the January control run.

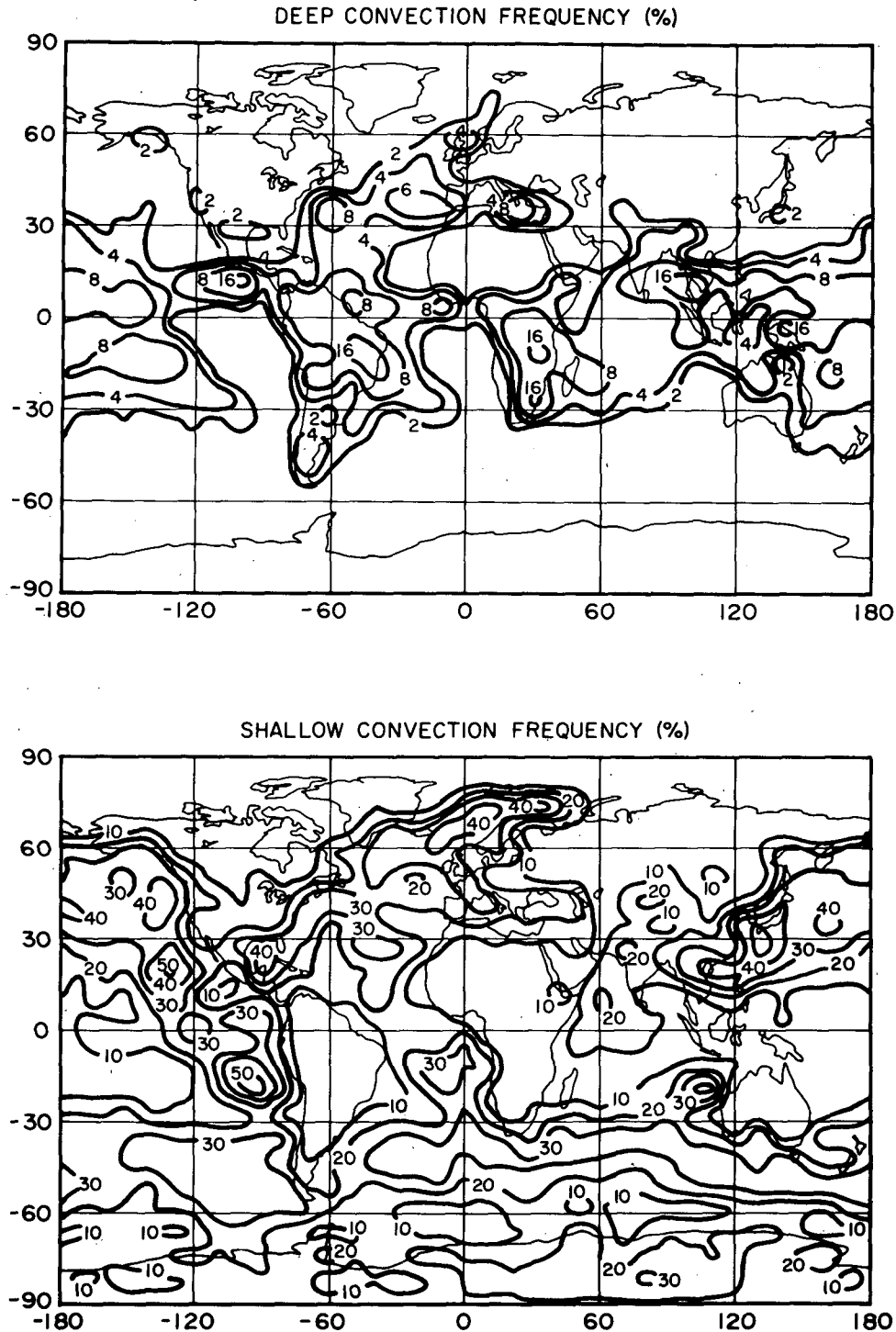


FIG. 2. Maps of the frequency of occurrence (in percent of GCM physics time steps) of deep convection (defined as all events that penetrate at least 4 GCM levels) and shallow convection (defined as all events that penetrate no farther than GCM level 3) for the control run.

mulus mass flux in Model II is too small or the arbitrary mass flux per event is much too large. We will argue for the latter interpretation in the next section. Shallow convection frequencies (the percentage of time steps

with convective events with cloud tops at or below model level 3) are generally higher and more randomly distributed, but with qualitatively realistic maxima in the marine trade cumulus and stratocumulus regions

off the west coasts of North America, South America, Africa, and Australia (Fig. 2b).

3. Results

a. Convection distribution and heating

Changes in the zonal-mean cumulus mass-flux profiles are displayed in Fig. 3 as differences between successive experiments. Experiment W, which ties convection to large-scale lifting, produces much less convective mass flux in the monthly mean than the arbitrarily determined control (see also Table 1). Much of the change is at low levels, but significant decreases also occur in tropical deep events, including a desirable shift in the mass flux peak from 12°N to the equator. Spurious high-latitude, upper-level events are also practically eliminated. The addition of the surface flux term (Experiment S) gives a global mean cumulus mass flux about halfway between those of Experiment W and the control but effectively cancels the low-latitude effects of Experiment W. This suggests that the surface flux influence on convection is too great in both Experiment S and Model II, although the relationship is implicit in the latter. Varying PBL height (Experiment Z) slightly increases M_c at low levels but generally has very little effect on this and most other aspects of the simulation. Downdrafts (Experiment D), on the other hand, enhance deep convection at the equator by re-supplying moisture to the PBL relative to Z, partially offsetting the drying of environmental subsidence.

Changes in the geographical distribution of convection occurrence frequencies are compared in Figs. 4 and 5. The average mass exchange per convective event in Experiment W is about 5% of the cloud base grid box (2.5 mb h^{-1}) in the ITCZ. This value is slightly less than estimates diagnosed from GATE data (Johnson 1980) but a good deal more realistic than the 50% prescribed in the control. Since less mass rises in each event, Experiment W convects much more often than the control despite its smaller time mean cumulus mass flux. Increases in convective events are largest in areas of strong convergence such as the ITCZ and midlatitude storm tracks. Shallow convection, on the other hand, decreases almost everywhere, but especially in the marine trade cumulus and stratocumulus regions where large-scale subsidence is prevalent.

Globally, Experiment S produces more frequent deep convection than Experiment W, but the increases are confined to the continental and warm ocean regions of the ITCZ. Colder tropical oceans and midlatitudes actually show less frequent deep convection but much more shallow convection. Varying PBL height (Z) essentially keeps the time mean mass flux the same by producing fewer events of both types with greater mass flux per event. The effect of downdrafts (D) is to enhance deep convection throughout the ITCZ and shallow convection in colder ocean regions. Deep convection frequencies in the ITCZ in Experiment D are typ-

ically 40%–70% and the mass flux per event is about 5 mb h^{-1} , both close to observations (Del Genio and Yao 1987; Johnson 1980).

Since the downdrafts that result from the parameterization used in Experiment D are not constrained to originate at a particular altitude or within a particular type of cumulus cloud, it is interesting to examine the conditions that favor their formation. Figure 6 shows the frequency of occurrence of downdrafts as a function of the cloud base and cloud top levels of the updrafts that give rise to them. It can be seen that downdrafts are most often associated with deep convective events (cloud top level \geq cloud base level) whose cloud base level lies in the PBL, because such events are most likely to mix cloudy air with cold, dry, midtroposphere air, which is conducive to the generation of negative buoyancy. As a result, convective events with downdrafts occur preferentially in the tropics in a January simulation (Fig. 7). Figure 7 also shows that oceanic events are somewhat more likely to produce downdrafts than continental events. This is probably due to the higher humidity of the marine PBL, which produces plumes with greater liquid water content and therefore greater potential for evaporative cooling. The downdrafts themselves tend to originate within the lower and middle portions of the updraft, primarily at the 786 mb and 634 mb levels (not shown) where environmental moist static energy is a minimum. This is consistent with available observations (Houze and Betts 1981; Knupp and Cotton 1985) and recent mesoscale simulations (Tao et al. 1987), suggesting that our simple parameterization captures at least some of the essential physics of downdrafts.

A challenge for any moist convection scheme is its ability to simulate vertical profiles of cumulus heating. Figure 8 illustrates the effect of different parameterizations at four grid points representing different convective regimes. In the Marshall Islands region of the western Pacific ITCZ, the control run predicts much weaker heating than the observed peak value of 5°C d^{-1} (Reed and Recker 1971; Thompson et al. 1979). Convergence-based convection greatly increases the heating, while the addition of surface fluxes (Experiment Z is shown; Experiment S gives a similar result) produces heating even weaker than the control. Downdrafts significantly increase cumulus heating in this region; in fact, another experiment with downdrafts but without varying PBL height produces peak heating equal to that observed. All of the runs exhibit excessive lower troposphere heating, a possible reflection of either the GCM's simple condensate reevaporation formulation or its representation of shallow convection. However, considering that the simulation is for a different season and different large-scale meteorological conditions than the observations, the results for several of the runs are encouraging.

At a continental ITCZ grid point (central Africa), the dependence of cumulus heating on mass flux pa-

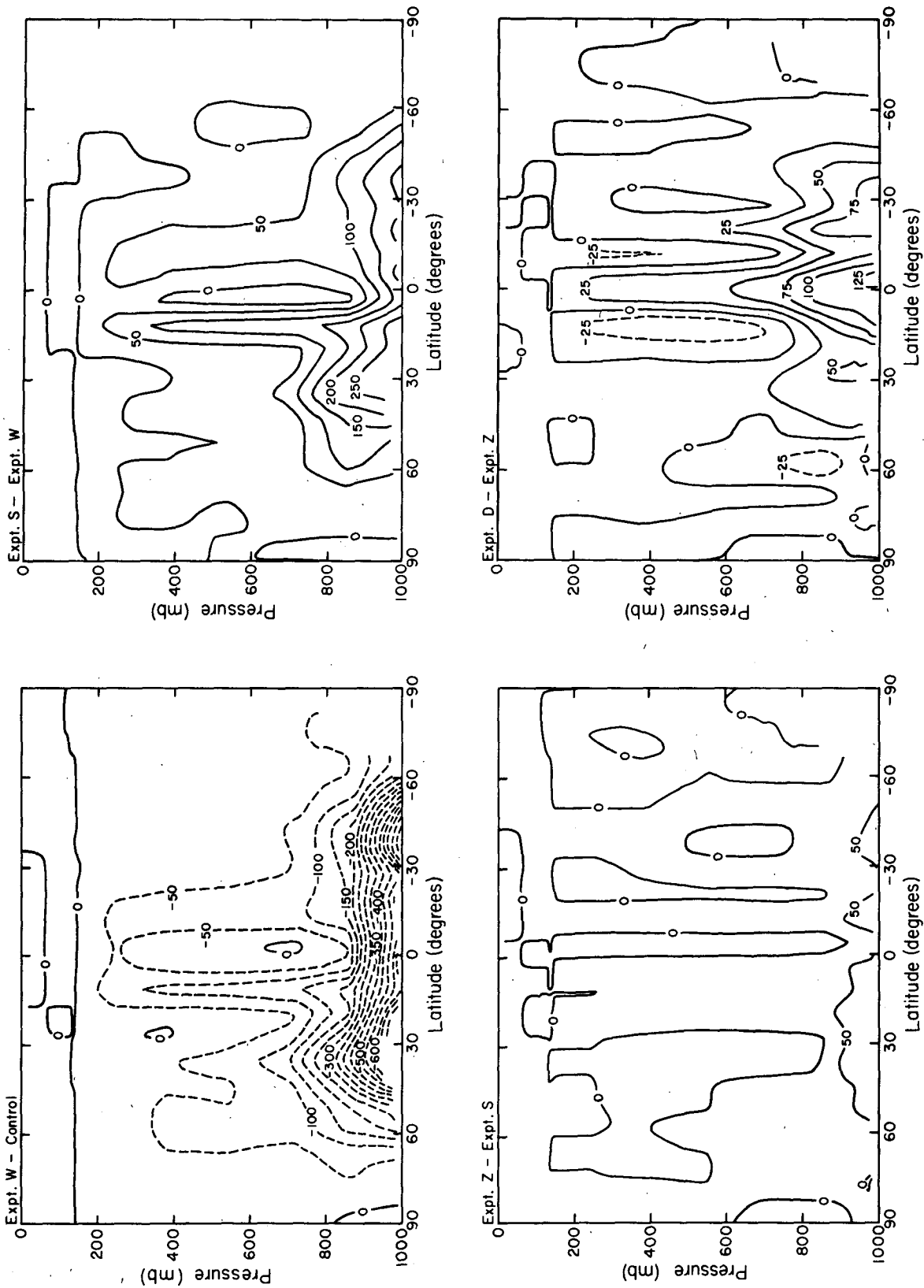


FIG. 3. Differences in zonal mean cumulus mass exchange between various runs: Experiment W minus control (upper left), Experiment S minus Experiment W (upper right), Experiment Z minus Experiment S (lower left), Experiment D minus Experiment Z (lower right). Units in 10^9 kg s^{-1} .

TABLE 1. Zonal mean diabatic heating and general circulation quantities for all the experiments.

	Experiment				
	Control	W	S	Z	D
Cumulus mass exchange (10^9 kg s^{-1})					
Global	1868	665	1246	1334	1473
Equator	150	104	125	128	168
Atmospheric diabatic heating (W m^{-2})					
Radiation	-118	-117	-115	-115	-116
Convection	88	56	76	79	78
Large-scale condensation	9	32	16	14	14
Sensible	23	31	26	25	25
Total	1.8	1.5	1.7	1.6	1.6
Peak N.H. streamfunction (10^9 kg s^{-1})					
Hadley cell	149	139	144	146	139
Ferrel cell	3	6	7	12	10
Vertically averaged vertical velocity $12^\circ\text{N}-12^\circ\text{S}$ ($10^{-5} \text{ mb s}^{-1}$)	7.2	6.5	7.0	7.0	6.5
Peak N.H. zonal wind					
Magnitude (m s^{-1})	39.9	37.6	35.8	34.9	35.4
Latitude (deg.)	23	23	23	23	31
N.H. tropospheric energy (10^5 J m^{-2})					
Eddy kinetic (EKE)	11.9	12.3	12.0	11.7	12.1
Zonal kinetic (ZKE)	7.4	6.7	6.8	6.7	6.8
Available potential (APE)	74.9	78.7	75.3	76.9	75.2
N.H. energy conversions (W m^{-2})					
APE \rightarrow EKE	1.7	1.6	1.5	1.7	1.6
EKE \rightarrow ZKE	-0.1	-0.2	-0.2	-0.0	-0.0
APE \rightarrow ZKE	0.9	0.8	0.9	0.8	0.7
Poleward transports (N.H.)					
Eddy: dry static energy (10^{14} W)	16	16	16	16	15
latent heat (10^{14} W)	14	13	14	14	16
angular momentum (10^{18} J)	5	7	5	10	7
Mean: dry static energy (10^{14} W)	22	23	26	24	26
latent heat (10^{14} W)	-9	-10	-9	-10	-11
angular momentum (10^{18} J)	3	3	5	4	5
Upward transports (global)					
Eddy: dry static energy (10^{14} W)	28	30	29	28	27
latent heat (10^{14} W)	32	35	31	31	33
angular momentum (10^{18} J)	-4	-3	-4	-3	-3
Mean: dry static energy (10^{14} W)	21	12	19	17	18
latent heat (10^{14} W)	-4	3	4	4	5
angular momentum (10^{18} J)	56	44	51	50	51

parameterization is just the opposite of that seen in the oceanic ITCZ. Convection tied to large-scale lifting decreases and surface moisture fluxes greatly enhance the moist convective heating rate, while downdrafts have little effect. This comparison illustrates the difficulty involved in designing a cumulus parameterization that is appropriate for all types of convective situations; we will return to this point in connection with the diurnal cycle in section 3e.

The situation in regions dominated by shallow convection is more straightforward. At a grid point in the Hawaiian Islands region where trade cumulus are prevalent, the model predicts cumulus heating that peaks near the top of the PBL (Fig. 8). Because this area is dominated by large-scale subsidence, Experiment W produces extremely weak heating, while surface fluxes increase the heating to 2.3°C d^{-1} , consistent

with that observed in a similar region of the Atlantic trades during BOMEX (Esbensen 1975). In the South Atlantic off the west coast of Africa, where conditions are even more suppressed and marine stratocumulus dominate, the dependence on mass flux parameterization is similar but heating rates are weaker. In both regions, downdrafts are rare (because our parameterization favors downdraft formation in deep events; see Figs. 6, 7) and therefore have little impact on the heating rate.

b. Hydrology and temperature

The precipitation patterns produced by the various experiments are consistent with the changes in the cumulus mass flux and deep convection frequency distributions (Figs. 3, 4). Figure 9 compares the precip-

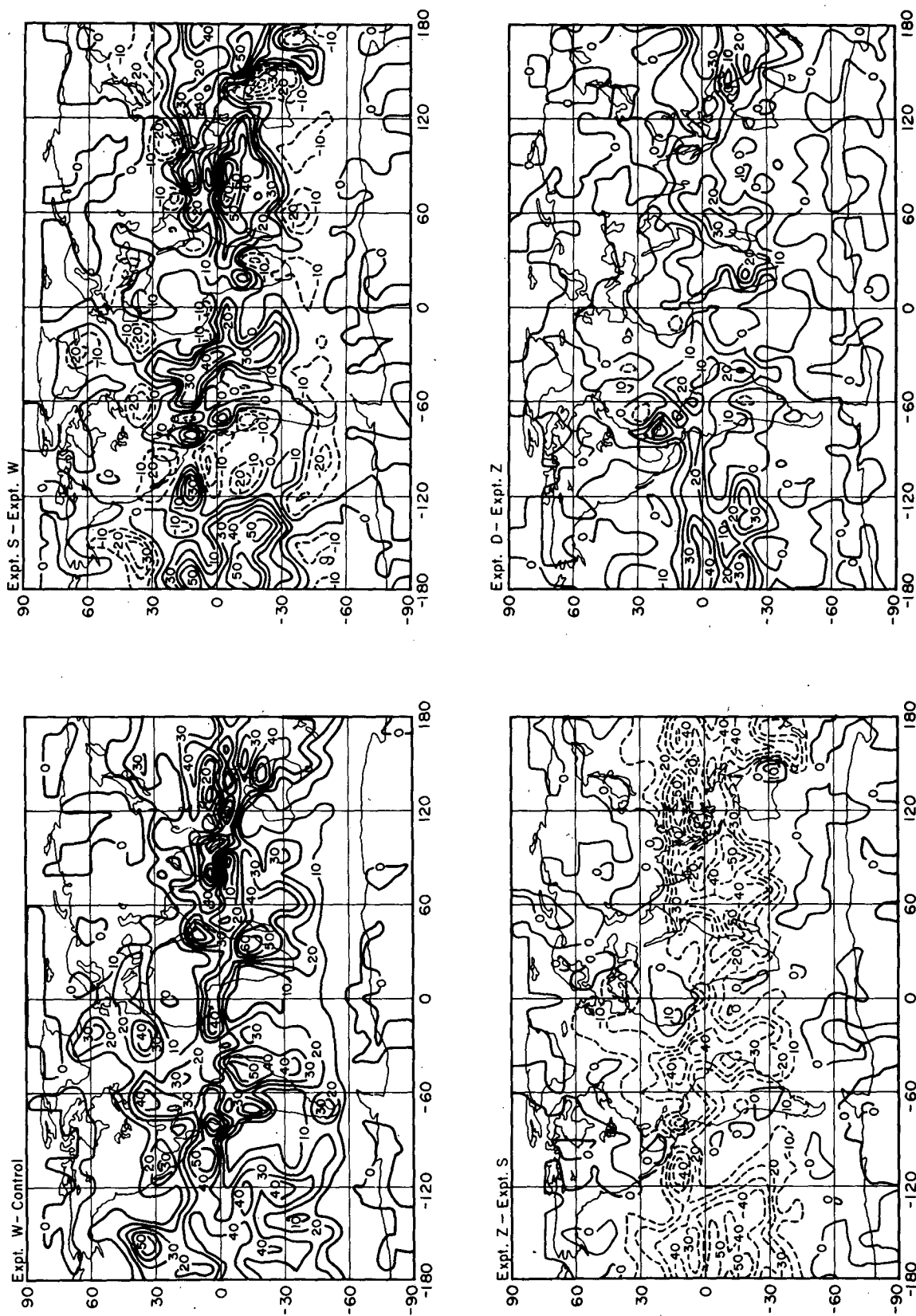


FIG. 4. As in Fig. 3 but for differences in the geographical distribution of deep convection occurrence frequency (%).

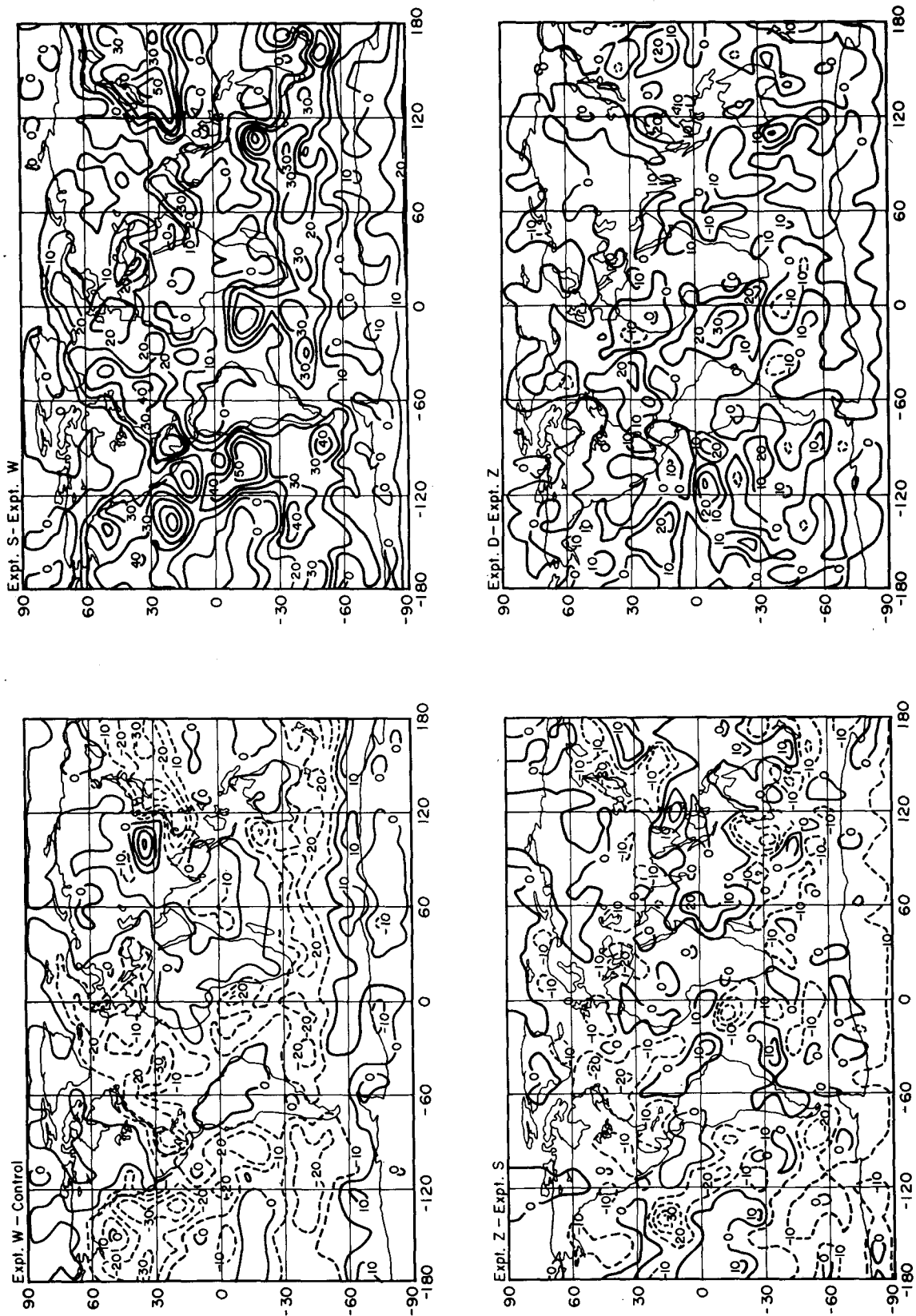


FIG. 5. As in Fig. 4 but for differences in shallow convection frequency.

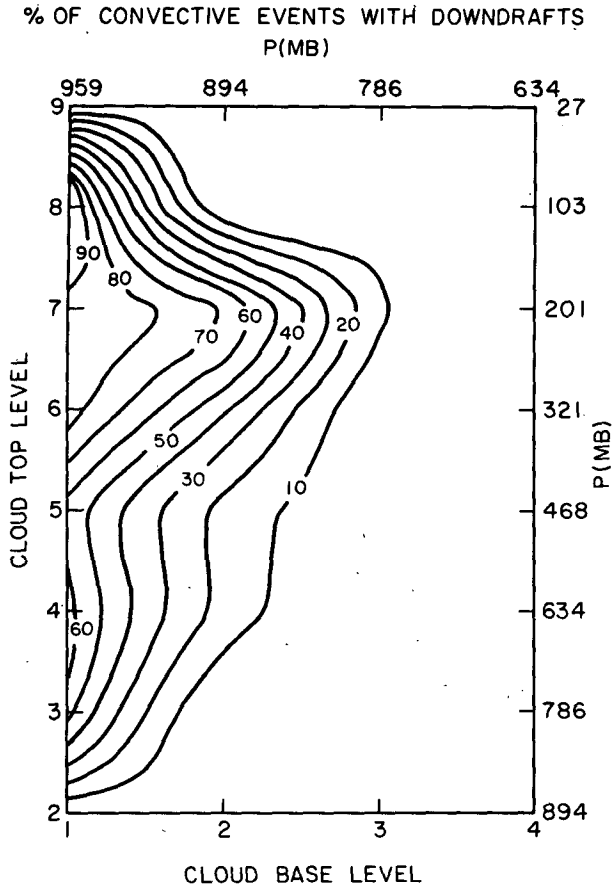


FIG. 6. Percentage of convective events in which downdrafts occur as a function of updraft cloud base and cloud top GCM levels (with corresponding pressures on opposite axes) for the last day of Experiment D. The time period sampled represents an ensemble of almost 3900 deep convective events globally and more than 800 at equatorial grid points.

itation field for the control run with that from Experiment D. The experiment produces a generally sharper Pacific ITCZ and better separation between the ITCZ and SPCZ. It also removes the precipitation anomaly off the Central American coast and greatly reduces precipitation over the India/Bay of Bengal region and Indochina. The zonal mean precipitation peak shifts from 12°N to 4°S, in accord with existing January precipitation climatologies (Jaeger 1976). The changes are due in part to the convergence dependence of the mass flux and in part to the downdrafts. The latter are actually necessary to counter the tendency of the surface fluxes to generate rainfall at 12°N in the model. However, the surface flux contribution cannot be removed, since it is largely responsible for the realistic precipitation values over South America and Africa.

Atmospheric moisture is a crucial diagnostic for climate models because it affects water vapor feedback, large-scale cloud feedback, moist static instability (and thus precipitation), and tropospheric chemical reactions. Moist convection is probably the controlling factor for humidity throughout the tropics and within the PBL at higher latitudes. That this is so is demonstrated by Fig. 10, which shows the changes in relative humidity caused by the different mass flux prescriptions in our experiments. The greatly diminished convection of Experiment W reduces upward moisture transport, drying out the tropical middle troposphere and moistening the PBL all the way up to midlatitudes; Experiment S, with its stronger convection, cancels much of this effect. Varying PBL height is not a factor for the moisture field, while downdrafts significantly moisten the equatorial PBL relative to a simulation with only dry subsidence, as expected. The PBL relative humidity in Experiment D is about 90% over the tropical oceans, consistent with GATE data (Thompson et al. 1979).

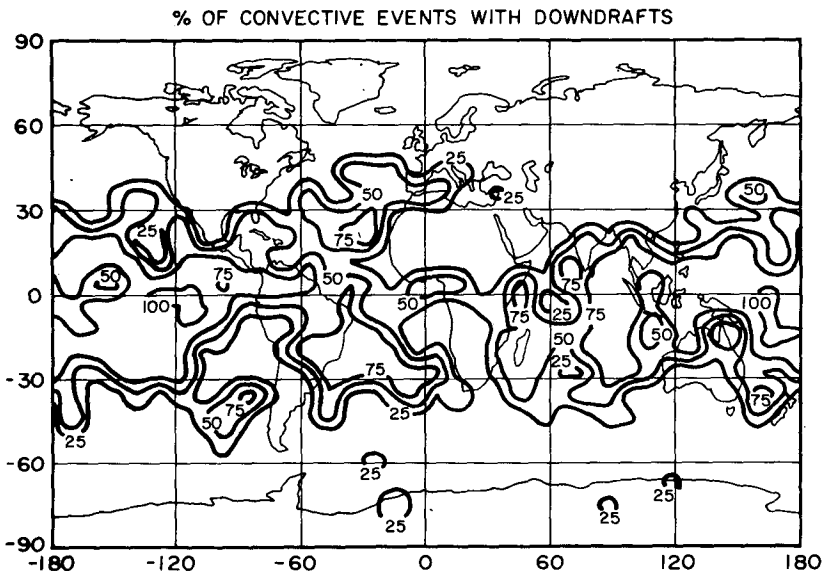


FIG. 7. Geographical distribution of the percentage of convective events with downdrafts for the last day of Experiment D.

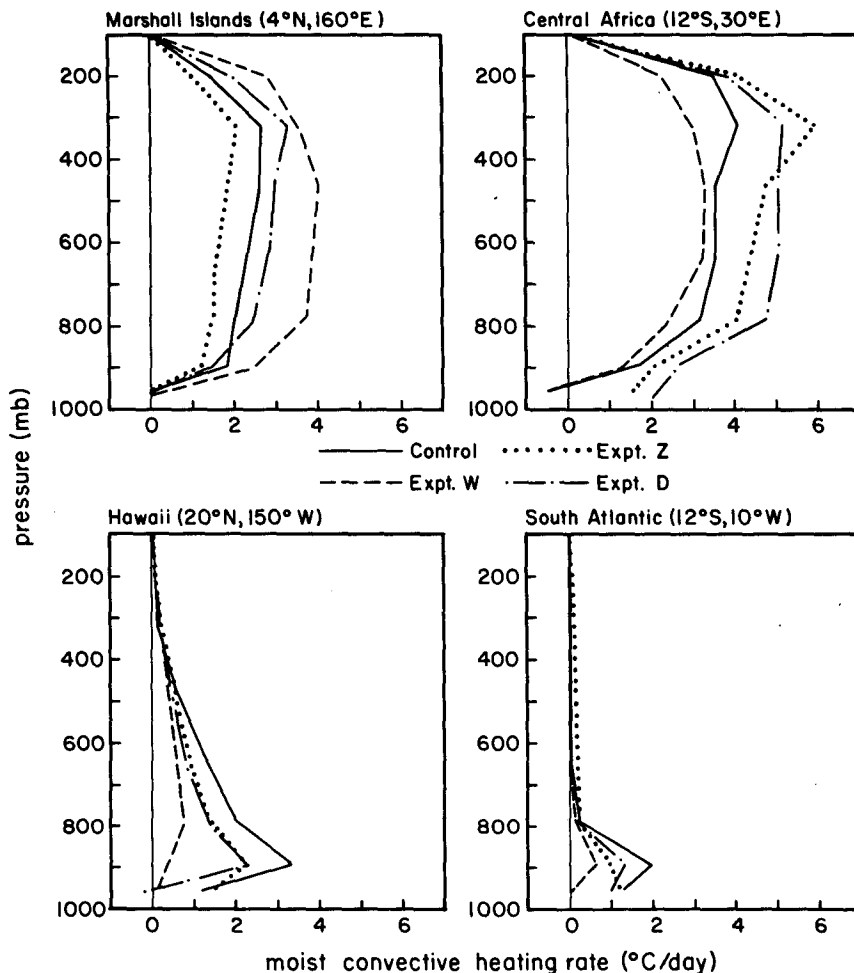


FIG. 8. Vertical profiles of cumulus heating rate at selected grid points for four of the experiments.

Although temperature varies in the experiments (see Fig. 11 and discussion below), the relative humidity changes largely reflect changes in specific humidity. For example, at 4°N , q at the lowest three GCM levels (959, 894, and 786 mb) increases from 14.2, 10.5 and 7.3 g kg^{-1} , respectively, in the control to 15.2, 11.3 and 8.0 g kg^{-1} in Experiment D (compared with observed values of 14.7, 11.8 and 8.0 g kg^{-1} estimated by interpolation from Oort 1983). The ability of our downdraft experiment to produce realistic low-level humidity may explain why penetrative schemes with only environmental subsidence tend to excessively dry out the lower troposphere (Geleyn et al. 1982). Unfortunately, the desirable midtroposphere drying caused by convergence limitations on cumulus mass flux extends only up to the 500 mb level. A separate experiment that limits condensate reevaporation to pressures greater than 500 mb has only a small effect on the 200 mb humidity. This suggests that further reductions in the cumulus mass flux, at least in the upper troposphere, may be necessary to produce an accurate humidity profile in the GISS model.

Temperature changes (Fig. 11) and cloud cover changes (Fig. 12) are intimately related to each other as well as to changes in convective heat and moisture transports. Once again, Experiments W and S are almost mirror images in their effects; the decreased (increased) convection in the former (latter) cools (warms) the troposphere by as much as 5 K. Temperature effects are actually greatest in the subtropics, probably because of the dramatic changes in shallow convective mass flux (Fig. 3). Low cloud cover changes in these runs apparently follow changes in the specific humidity more so than temperature, as can be seen by comparing Figs. 10–12. High cloud changes in the tropics, on the other hand, are opposite to that expected from changes in q and seemingly better correlated with local temperature changes. Neither of the other experiments produces large changes in either temperature or cloud cover by comparison, although downdrafts cause small increases in tropical cloudiness at most levels and a slight cooling of the PBL relative to the midtroposphere. In general, changes in convective cloudiness are out of phase with changes in large-scale

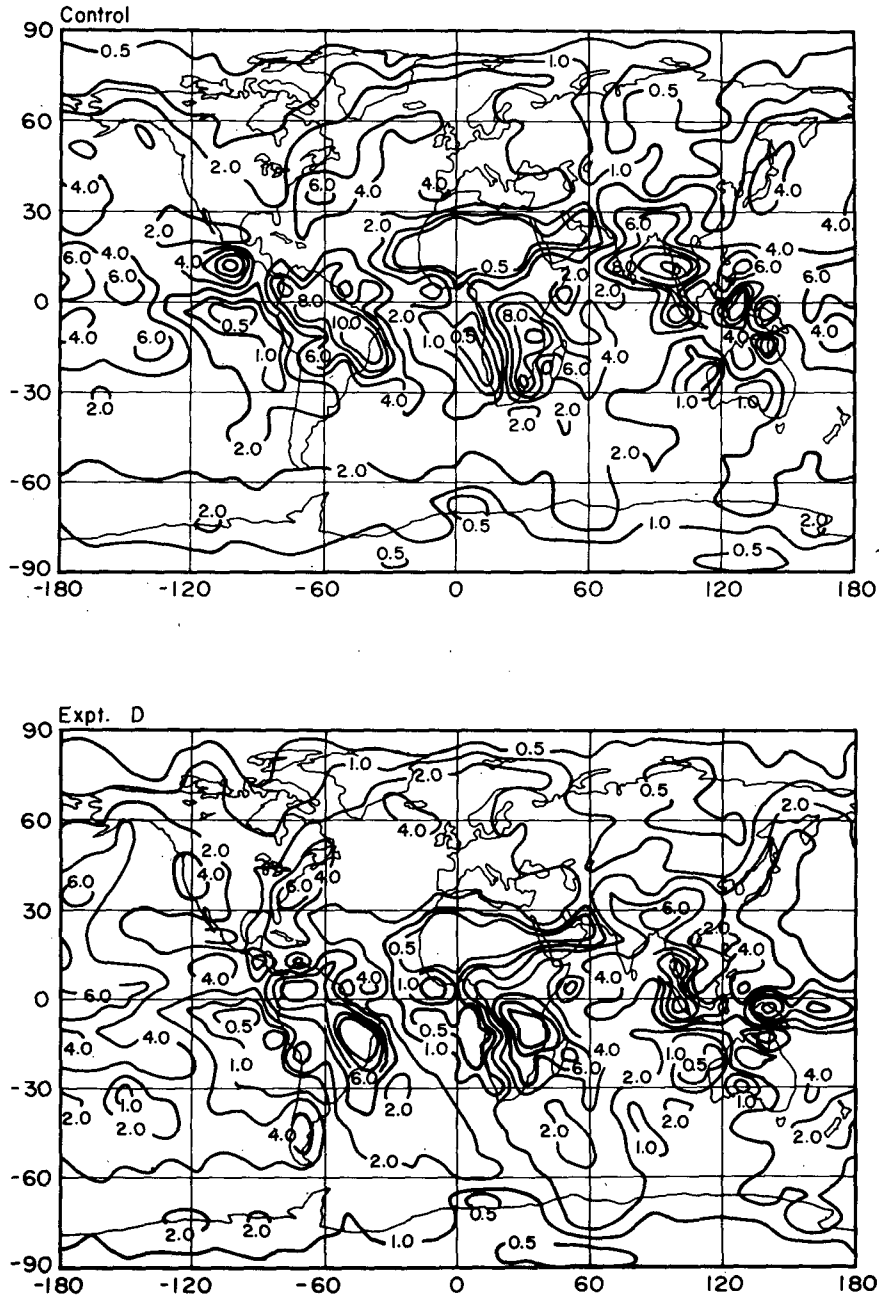


FIG. 9. Geographical distribution of precipitation (mm d^{-1}) for the control run (upper) and for Experiment D (lower).

supersaturation clouds in the experiments, with the latter usually determining the change in total cloud cover.

c. General circulation

Moist convection is much touted as a forcing function for the general circulation of the atmosphere. Considering the gross changes that occur in the magnitude and latitudinal distribution of cumulus mass

flux in our experiments, one might therefore expect corresponding dramatic dynamical changes. However, this is generally not the case, at least for zonally averaged aspects of the circulation. Table 1 compares a number of standard indicators of the general circulation for each of the experiments. A few general tendencies can be seen, e.g., a slight weakening of the Hadley cell in response to weaker convection and a strengthening of the Ferrel cell as poleward angular momentum transport increases. For the most part, though, these

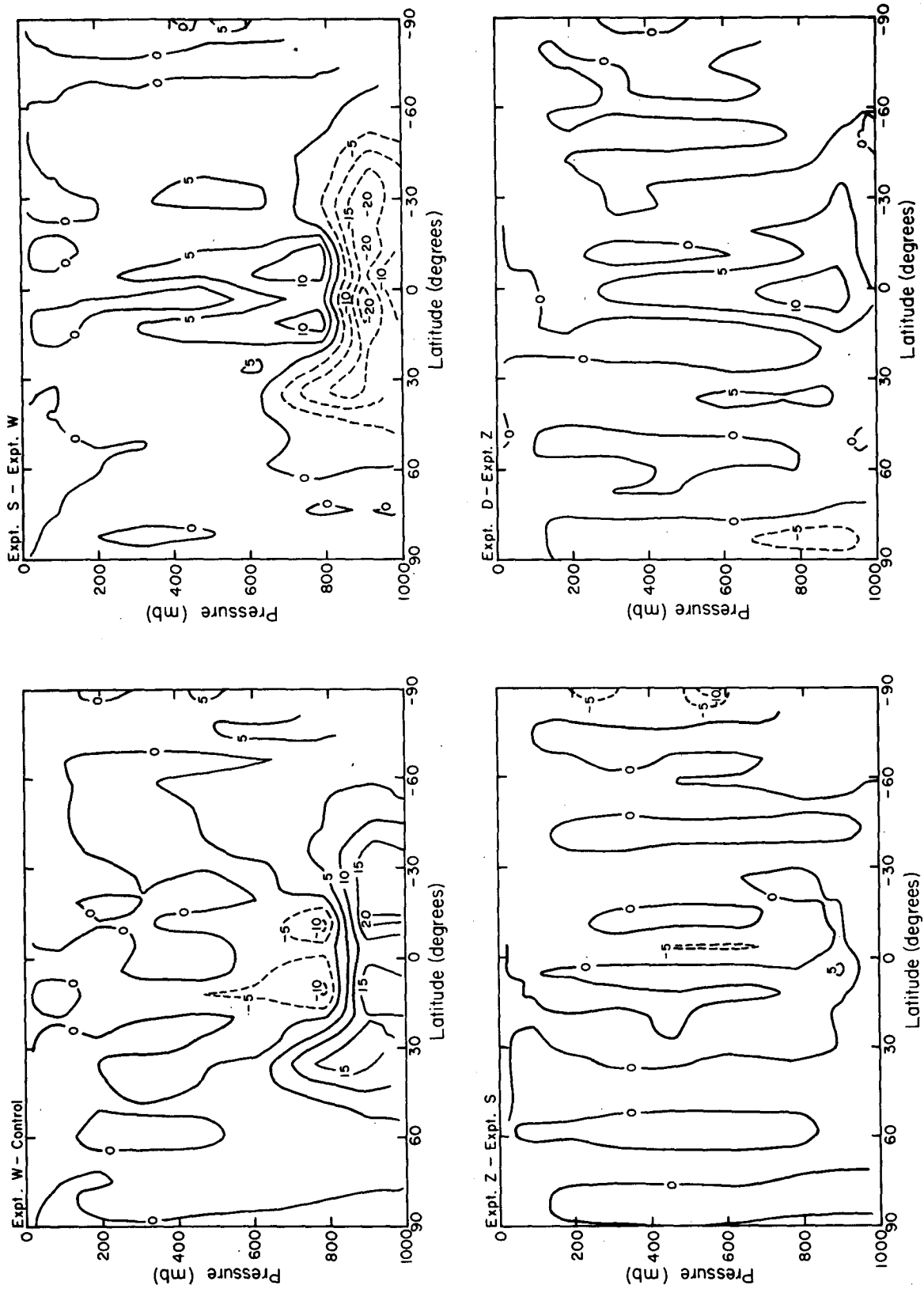


FIG. 10. As in Fig. 3 but for differences in relative humidity (%).

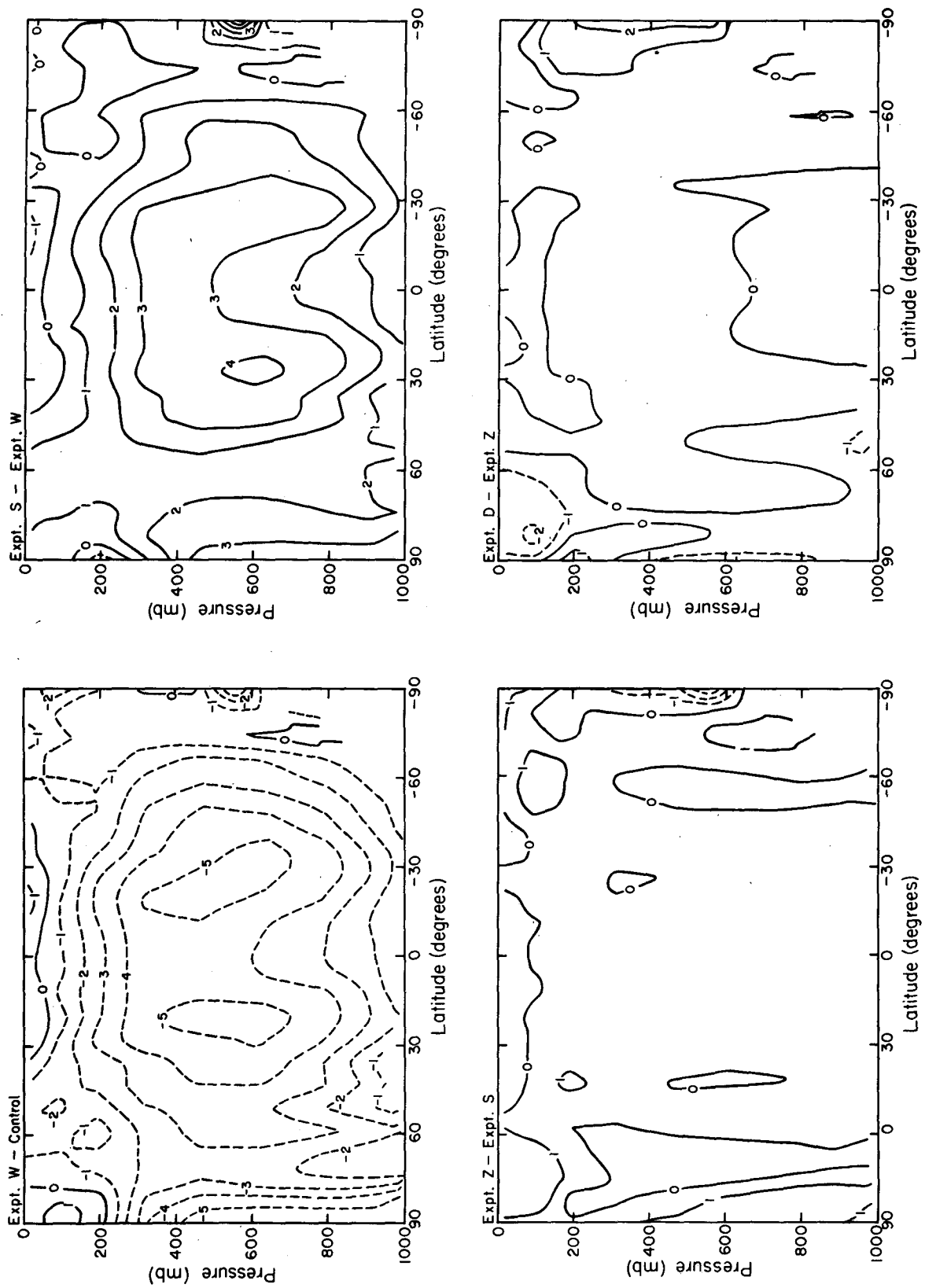


FIG. 11. As in Fig. 3 but for differences in temperature ($^{\circ}\text{C}$).

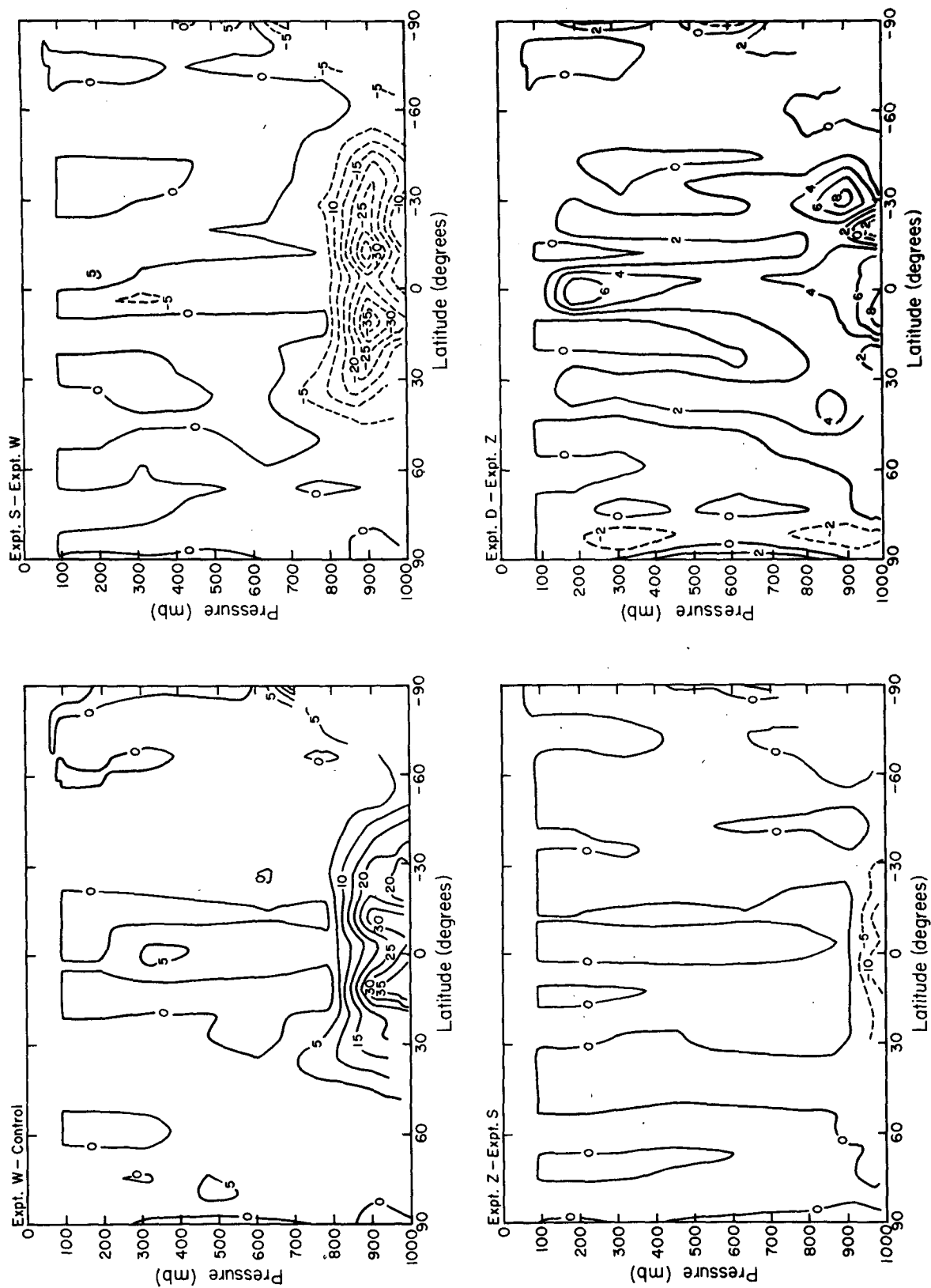


FIG. 12. As in Fig. 3 but for differences in total cloud cover (%).

and other differences are smaller than or comparable to the model's intrinsic interannual variability. Baker et al. (1977), by comparison, noted significant differences in the energy cycle of the NCAR GCM when a Kuo scheme was substituted for the standard convective adjustment used in most versions of the model. This difference in sensitivity may reflect the fact that our experiments differ less from each other than do the schemes compared by Baker et al. Donner (1986) has described the very different thermal balances produced by these parameterizations, while Albrecht et al. (1986) have pointed out the inadequate treatment of moisture fluxes in the convective adjustment approach.

The insensitivity of the general circulation to changes in convection in our experiments is due in part to the response of other diabatic processes to changes in cumulus heating. Table 1 also shows the components of the global atmospheric diabatic heating. Cumulus heating changes in the experiments are significant but less dramatic than changes in cumulus mass flux, because the mass flux includes shallow convective events that release little latent heat. At the equator, in fact, column convective heating varies even less from one experiment to the next because low-level humidity variations (Fig. 10) regulate condensate reevaporation in such a way as to cancel variations in updraft latent heat release. Globally, convective heating variations are offset by changes in large-scale condensation and surface sensible heating, keeping the total diabatic heating almost constant. This compensation may, in part, be a function of the fixed SST in the experiments. It is interesting to note that the vertically integrated radiative heating plays almost no role in the compensation process, despite the large cloud cover changes in several of the experiments (Fig. 12). (However, the vertical profile of radiative heating does change, so radiation is involved in local compensation.) This result suggests that cloud/radiation/dynamics feedbacks may be more complex than the simple radiative-convective adjustment implied by the study of Albrecht et al. (1986), which involved only changes in the vertical distribution rather than in the magnitude of convective heating. Of course the feedbacks seen in our experiments are responses to changes in one parameter within the same basic parameterization (except for Experiment D). Different results may occur when completely different schemes are compared (cf. Donner 1986).

A second factor limiting the sensitivity of the GCM to variations in moist convection strength is the compensation provided by large-scale dynamic transports. This compensation is most evident in the vertical budgets of heat, moisture and momentum (Table 1). The largest changes in vertical transports are associated with Experiment W, which has only 36% as much cumulus mass flux globally as the control. With less downward transport of dry static energy by convection, there is less upward transport by the large-scale dynamics in Experiment W. The burden for this is borne completely

by the mean flow—upward eddy transport actually increases. Similarly, with less upward convective moisture flux, there is a larger dynamical flux. In this case, however, compensation is due to increased upward eddy transport. Finally, with less cumulus friction in Experiment W, the mean flow adjusts by transporting less angular momentum upward. The common thread is weaker transport by the mean meridional circulation (even though the decrease in Hadley cell streamfunction is itself only marginally significant).

Our results are consistent with the findings of Rind and Rossow (1984) and Rind (1986) that the feedbacks among various dynamical processes limit the response of the general circulation in climate change experiments. If the large-scale dynamics is relatively insensitive to climate change, and convection is tied to the dynamics (e.g., via the dependence of M_c on w_B), then we expect the response of convection to climate change to be weaker than estimates from previous doubled CO_2 experiments, which relate convection only to the existence or degree of moist static instability. We will return to this point in section 4a.

The response of the GCM's circulation to changes in moist convection is quite different when we focus on deviations from the zonally averaged flow, especially in the tropics. Figure 13 displays the model's upper and lower troposphere low-latitude zonal wind as a

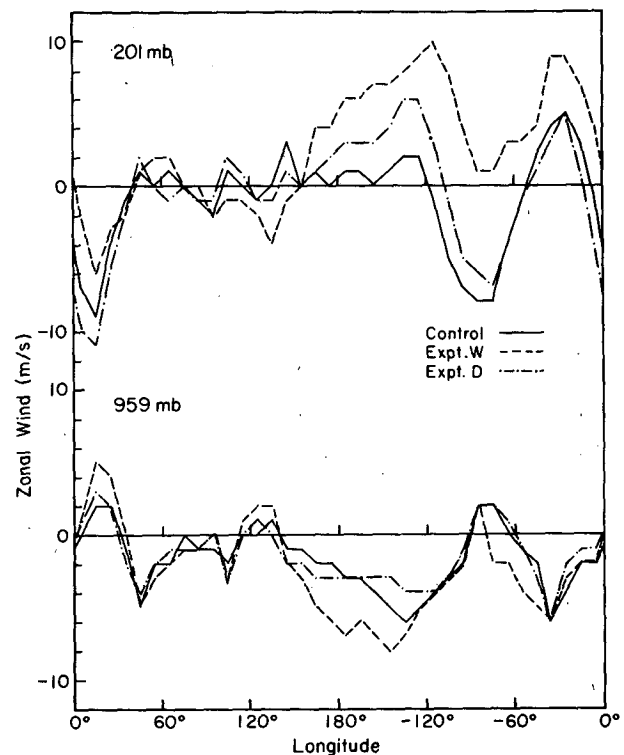


FIG. 13. Upper and lower troposphere zonal wind in the equatorial region (8°N – 16°S) as a function of longitude for three of the experiments.

function of longitude for several of the experiments (see also Fig. 17 and the discussion in section 4b). The Walker circulation associated with rising motion in the western Pacific and Indonesia is evident in the transition from easterlies to westerlies at 201 mb just west of the dateline and vice versa at 959 mb. A similar pair of cells tied to heating over South America can be seen centered at -50° . The control produces a relatively weak signature of the Walker cell in its upper level westerlies. Experiment W, which ties cumulus mass flux to convergence, gives the strongest Walker circulation but a zonal mean zonal wind at 200 mb which is too westerly, although its PBL zonal winds are fairly realistic. Experiments S and Z (not shown) are similar to the control, while the downdraft experiment strengthens the circulation somewhat relative to Experiment Z.

The western Pacific component of the Hadley circulation is also strengthened in the sensitivity experiments, albeit to a lesser extent. In the control run, upper level divergence is equally partitioned between the Hadley and Walker components of the circulation. In Experiments W and D, though, perturbation westerlies in the western Pacific at 201 mb are double their magnitude in the control, while the peak average meridional wind between 165°E and 155°W increases from 2.8 m s^{-1} in the control to 3.4 m s^{-1} in Experiment W and 3.7 m s^{-1} in Experiment D.

The better definition of the Walker circulation is a result of more large-scale organization of the tropical convection in the sensitivity experiments. This is illustrated by Fig. 14, which shows the equatorial eddy kinetic energy spectrum for several runs. The control is globally deficient in tropospheric longwave eddy energy in comparison to observations (Saltzman 1970) and does not exhibit the observed wavenumber 1 peak in the tropics (Julian et al. 1970). The experiments slightly exacerbate this problem in midlatitudes (although meridional transports are not affected). However, Fig. 14 shows that longwave eddy energy is significantly enhanced at the equator in all the experiments because convective events are not as randomly distributed as in the control. This result suggests that the convection schemes described here may help augment interhemispheric mixing of trace gases, a weakness of Model II (Prather et al. 1987). Much of the longwave increase is in transient waves: Experiments W and D have 35% and 46% more transient eddy kinetic energy in wavenumbers 1–3 than the control. This may be an indication of wave-CISK feedbacks operating on model-generated Kelvin and mixed Rossby-gravity waves.

d. Energy balance

Components of the global atmospheric energy balance at the top of the atmosphere and the surface for each experiment are shown in Table 2. Changes in net

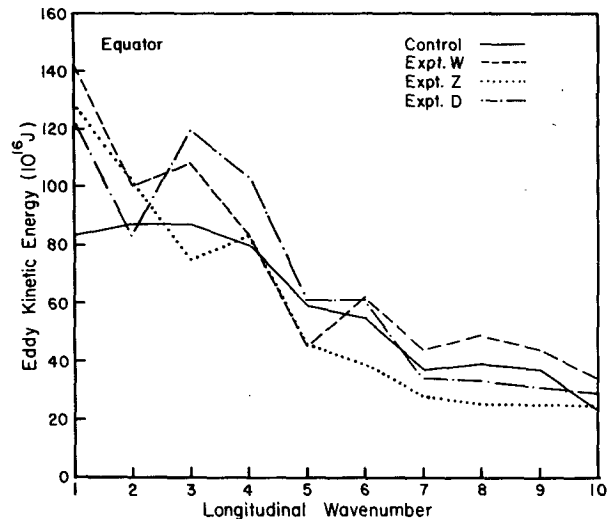


FIG. 14. Equatorial eddy kinetic energy spectrum for four of the experiments.

downward radiation at the top of the atmosphere are dominated by variations in shortwave absorption and scale directly with changes in the total cloud cover. Longwave variations due to atmospheric cooling or heating are secondary and anticorrelated with net radiation. The sensitivity of the radiation balance to clouds is illustrated by the most extreme experiment, W, which increases cloud cover by 10% and completely reverses the net planetary radiation. The most realistic experiment (D) reduces the global net radiation into the atmosphere by 2 W m^{-2} . Another experiment that includes a crude estimate of mesoscale cloud cover (by increasing convective cloud cover above 500 mb by a factor of 4 for deep convective events) further reduces the net planetary radiation by 3 W m^{-2} . We have not run this version of the model over the annual cycle, but the change in January net radiation suggests that the combined effect of downdrafts and mesoscale anvil clouds might remove most of the GCM's annual mean flux imbalance (cf. Hansen et al. 1984). Planetary albedo variations are also primarily cloud-related; ground albedo changes in the same sense (according to the surface temperature change) but to a much lesser degree.

Variations in the surface energy budget are tied to low cloud cover, which is responsible for much of the total cloud cover change. However, with the exception of Experiment W, shortwave variations do not always dominate the total change in net heating at the ground. All the experiments have weaker evaporation than the control, because the reduced convection maintains a higher relative humidity in the PBL. This is not true at all latitudes, though. Experiment W, for example, actually has more evaporation at the equator than the control because it focuses convergence there and increases the surface wind speed by 40%. Sensible heating

TABLE 2. Global mean climate quantities for all the experiments.

	Control	Experiment			
		W	S	Z	D
Net downward radiation into top of atmosphere ($W m^{-2}$)	15.2	-7.7	13.6	18.2	13.0
Absorbed shortwave	251.0	222.5	246.9	252.7	245.4
Net longwave	-235.8	-230.2	-233.3	-234.5	-232.4
Net downward energy flux into surface ($W m^{-2}$)	24.6	-3.0	21.8	26.6	21.5
Absorbed shortwave	182.4	152.9	178.1	184.1	176.4
Net longwave	-49.1	-43.3	-49.5	-50.6	-47.6
Sensible heat flux	-22.8	-30.7	-25.5	-24.6	-24.9
Evaporative heat flux	-84.7	-80.7	-80.2	-81.0	-81.1
Surface temperature ($^{\circ}C$)	12.0	10.7	11.5	11.9	11.8
Vertically averaged air temperature ($^{\circ}C$)	-21.6	-24.6	-22.6	-22.3	-22.2
Potential temperature difference, 468 mb-959 mb ($^{\circ}C$)	31.2	27.1	29.7	29.5	30.4
Vertically averaged specific humidity ($g kg^{-1}$)	2.44	2.17	2.36	2.42	2.53
Specific humidity difference, 959 mb-468 mb ($g kg^{-1}$)	7.55	8.78	7.80	7.75	7.87
Planetary albedo (%)	28.9	37.0	30.0	28.4	30.5
Ground albedo (%)	11.8	12.8	12.0	11.6	11.8
Total cloud cover (%)	45.1	54.9	45.7	43.1	46.4
High	21.4	22.2	22.6	21.8	23.2
Middle	15.2	16.2	16.7	16.4	18.0
Low	34.8	51.4	37.3	33.4	37.5
Mean cloud top pressure (mb)	475	541	474	456	457

increases in each run because weaker convective heating cools the atmosphere while sea surface temperatures are fixed in the experiments.

e. Diurnal cycle

One way to validate (or more likely invalidate, considering our current understanding of the climate system) a climate model is to test its response to known variations in forcing. The best documented of these are the seasonal and diurnal cycles. Simulation of the seasonal cycle is a comprehensive test of all elements of the model's dynamics and parameterized physics. Many elements of the climate system do not respond as much to the diurnal cycle, the notable exceptions being moist convection and the continental PBL. The highly variable nature of the diurnal cycle of convection from one geographic region to another suggests that convection must react to multiple forcings. From a climate standpoint, a GCM must correctly correlate clouds with diurnal insolation variations to produce a plausible cloud-radiation feedback. Consequently, the diurnal cycle of convection presents a crucial yet formidable challenge for any cumulus parameterization scheme.

Figures 15 and 16 illustrate the effect that cumulus parameterization can have on the diurnal cycle at typical continental and oceanic grid points in the tropics. Each figure compares the diurnal variation of precipitation and 200 mb cloud cover (which is often assumed to be correlated with moist convection), along

with two of the major forcing terms for convection (lifting and surface moisture flux), for two of the experiments. In the Sahel region of Africa (Fig. 15), convection should respond to the strong diurnal variation of PBL heating. When cumulus mass flux is parameterized in terms of both lifting and surface fluxes (Experiment S), this is indeed the case. Evaporation and upward motion both peak in the early afternoon, producing a distinct precipitation peak in the midafternoon, qualitatively correct but about three hours earlier than observed (McGarry and Reed 1978; Duvel and Kandel 1985; Del Genio and Yao 1987). High cloud cover is in phase with upper troposphere humidity and lags precipitation by four to five hours, in agreement with observations.

When cumulus mass flux is proportional only to convergence (Experiment W), however, large-scale vertical velocity actually peaks before dawn, out of phase with the afternoon sensible heating maximum. The precipitation peak weakens and shifts to midnight. This example of cloud/dynamics feedbacks gone awry emphasizes the importance of including some representation of the effects of surface fluxes in moist convection schemes.

In the western Pacific ITCZ, precipitation and very high cloudiness are observed to peak near dawn with a weaker diurnal amplitude than in continental areas (Gray and Jacobson 1977; Albright et al. 1985; Hartmann and Recker 1986; Fu 1988). Explanations of the early morning maximum include differential radiative cooling and subsidence between cloudy and

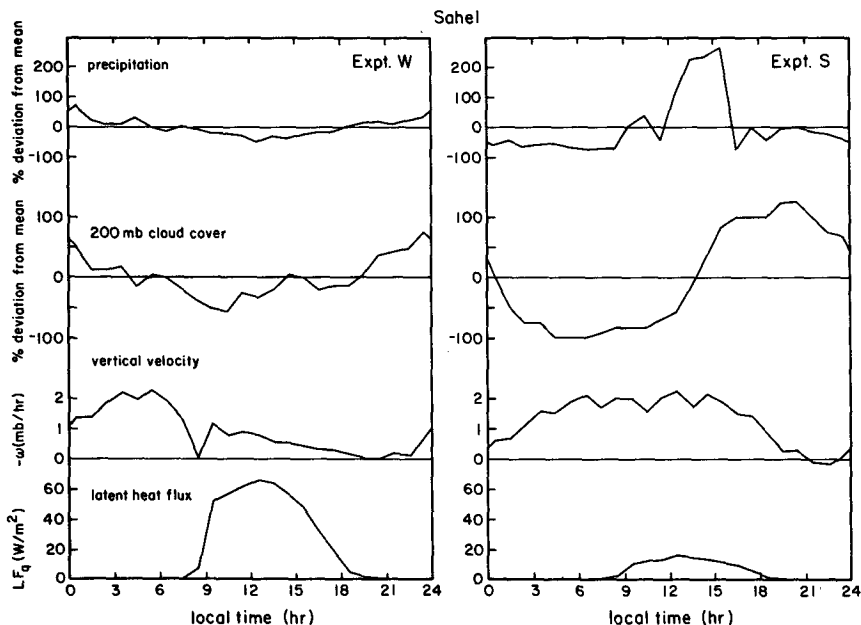


FIG. 15. Diurnal cycles of precipitation, 200 mb cloud cover, level 1 vertical velocity, and surface evaporative heat flux at a grid point in the Sahel region of Africa for two of the experiments.

surrounding clear regions (Gray and Jacobson 1977) and nighttime destabilization of the cloud top by radiative cooling (Hobgood 1986). In most cases, the GCM produces a midnight peak in precipitation in the Marshall Islands. However, when we parameterize cumulus mass flux in terms of convergence only (Experiment W), rainfall peaks several hours before dawn and minimizes near dusk (Fig. 16), in better agreement

with observations. The peak is roughly in phase with the maximum in vertical velocity, but the latter has a strong semidiurnal component and exhibits a secondary peak in late afternoon, when precipitation in the model is decreasing. High cloud cover variations are weak but more closely related to lifting than is precipitation. The cloud cover parameterization we use in these runs, which minimizes convective cloudiness,

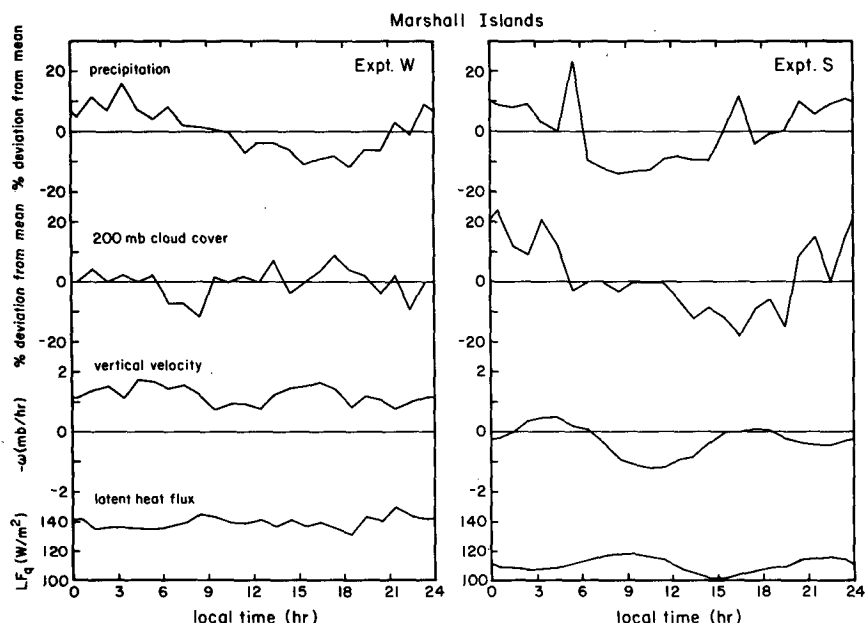


FIG. 16. As in Fig. 15 but for a grid point in the Marshall Islands region of the western Pacific.

limits the importance of either of the cloud-radiative feedbacks discussed above. Both mechanisms may therefore only enhance or slightly shift a diurnal cycle driven by other processes. When the surface flux contribution is added (Experiment S), the model shifts back to a general tendency for a midnight rainfall maximum and morning minimum, despite isolated sharp increases just before dawn and dusk. The isolated peaks roughly correlate with the semidiurnal peaks in lifting. Thus, the best parameterization for continental convection is not necessarily best for its oceanic counterpart.

4. Discussion

a. Implications for climate sensitivity

Cloud feedback is undoubtedly the single greatest source of uncertainty in estimates of the atmospheric contribution to climate sensitivity. Manabe and Stouffer (1980) inferred a climate sensitivity of 2°C at the surface for doubled CO_2 using a version of the GFDL GCM with moist convective adjustment and fixed clouds. A more recent version with predicted clouds warms the surface by about 4°C (Wetherald and Manabe 1986), as does the NCAR CCM with a similar cloud scheme (Washington and Meehl 1984). Hansen et al. (1984) produce a doubled CO_2 warming of 4.2°C with the GISS Model II GCM, which has penetrative convection and interactive clouds. Using a one-dimensional model, they estimate that 1.2°C of the warming results from changes in cloud cover and height and their nonlinear effect on other feedback processes in the GCM. The UKMO GCM, also with a penetrative convection scheme and predicted clouds, gives a 5.2°C response to doubled CO_2 (Wilson and Mitchell 1987).

The convection experiments described in this paper were conducted only for the current January climate and therefore do not simulate a radiative equilibrium state of the atmosphere, nor do they measure the convective response to forced changes in the equilibrium state. As a result, we cannot make quantitative statements about climate sensitivity on the basis of these runs alone. However, to the extent that the experiments represent realistic modifications of the moist convection parameterization in the GCM, we can attempt to qualitatively assess their effect on the cloud feedback predicted by Model II. In this regard, Experiment D is the most interesting. Its physics is the most comprehensive of all the experiments; furthermore, relative to Model II, it improves the simulation of deep convection frequencies and heating rates, precipitation patterns, the vertical humidity profile, Walker circulation, equatorial eddy kinetic energy, and net radiation. We thus consider the implications of all the experiments but focus especially on Experiment D and its combined effects of weaker convection (relative to Model II) and downdrafts. The complexity of convection/dynamics

interactions suggests, though, that such extrapolations be viewed circumspectly.

All the experiments produce significantly weaker convective mass fluxes than Model II (Fig. 3, Table 1). However, except for Experiment W, cloud cover changes are relatively small (Table 2). Low clouds are more sensitive than middle and high clouds to changes in convection strength, confirming the result of Hansen et al. (1984) that the former dominate the cloud cover contribution to the cloud/radiative feedback. Generally, low cloud cover anticorrelates with convection strength in our runs because convection removes moisture from the PBL faster than it can be resupplied by surface evaporation. Thus, we might anticipate that the feedback due to low clouds depends on how convection strength responds to doubled CO_2 .

In Model II fractional changes in convective heating for a variety of climate change experiments are almost identical to changes in surface evaporation (cf. Rind 1986, Table 1). Since the cumulus mass flux per event is fixed in Model II, changes in convection indicate only changes in the frequency of occurrence of deep moist static instability due to the altered evaporation. Similar arguments should hold for the GFDL, NCAR, and UKMO GCM doubled CO_2 experiments, except that the convective flux in these models also depends on the degree of instability. This difference is apparently not very important, considering the similar cloud feedback on global mean surface temperature in all of these models.

We have argued, though, that large-scale convergence is also an important determinant of cumulus mass flux. The fact that the tropical atmosphere often maintains itself in an unstable state until lifting triggers convection suggests that the convective response to doubled CO_2 will depend as much on changes in convergence as on changes in instability. The Hadley cell is a good indicator of tropical mean vertical motions in the GCM. In our experiments, the strength of the Hadley cell and the tropical mean vertical velocity are well correlated, and both are fairly insensitive to changes in convection (Table 1). In doubled CO_2 experiments with Model II, Hadley cell strength and mean vertical velocity in fact slightly decrease (Rind 1986). If M_c is explicitly linked to low-level convergence, the effect of increased surface fluxes on M_c in a doubled CO_2 experiment should therefore be muted if mean vertical motions do not respond in the same way. Taken at face value, this suggests that the response of the mean cumulus mass flux to doubled CO_2 will be less dramatic than that of Model II. We thus expect a smaller overall decrease in low clouds and a weaker positive feedback on global mean surface temperature due to changing cloud amount. This does not necessarily preclude regional changes in M_c . In fact, the sensitivity of the Walker circulation in our experiments (Figs. 13, 17) argues that the zonally asymmetric re-

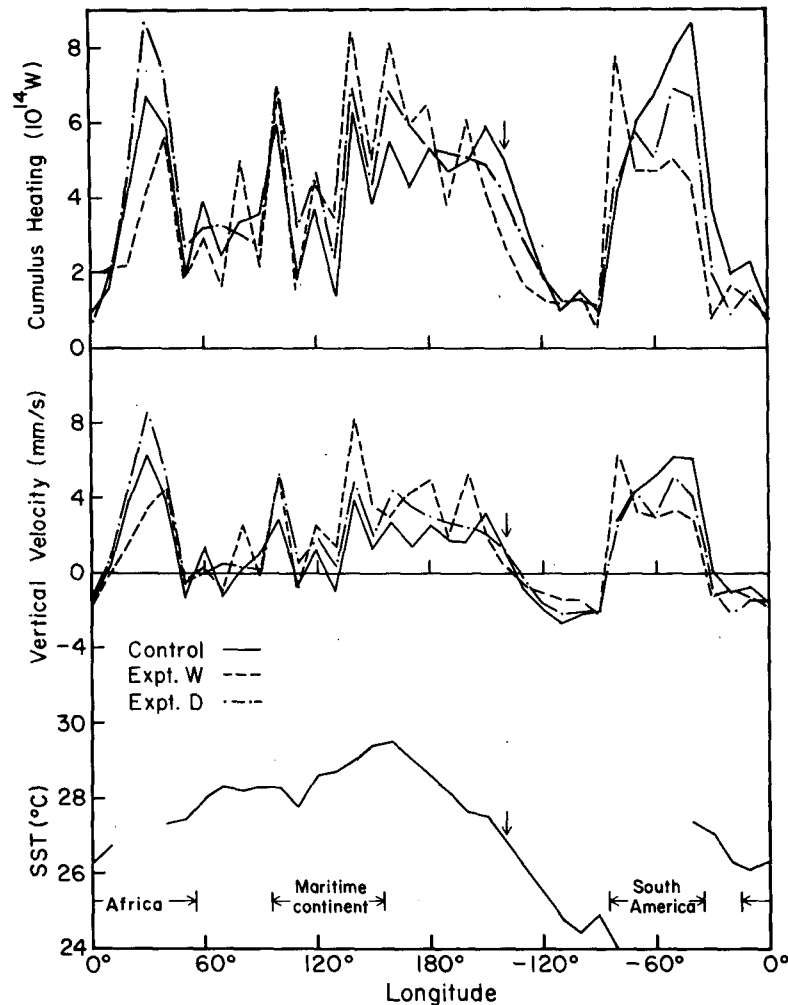


FIG. 17. Cumulus heating rate, vertically integrated vertical velocity, and sea surface temperature in the equatorial region (8°N – 16°S) as a function of longitude for three of the experiments. The longitudinal extent of full or partial land cover, representing Africa, the maritime continent, and South America, is indicated. Longitudes with missing SST data are fully land-covered. Arrows designate the 27°C SST longitude for the tropical Pacific.

sponse of convection to increased CO_2 may be quite important. Changes in the latitudinal and vertical dependence of the feedback are also likely.

The weaker cloud feedback we postulate due to convection/dynamics interactions is independent of other cloud feedbacks that can exist with or without changes in cumulus mass flux. Cloud optical thickness feedbacks (Somerville and Remer 1984; Betts and Harshvardhan 1987), for example, may work in the same direction, possibly even changing the sign of the net cloud feedback (Roeckner et al. 1987).

The impact of cloud height changes on cloud feedback is more difficult to diagnose. High and middle cloud variations are limited by cancellation between the effects of varying temperature and specific humidity

in the experiments. However, all the runs have more global mean middle and high cloud cover than the control, despite the fact that each one except Experiment D has less upper level moisture. This suggests that changing temperature rather than changing specific humidity controls variations in upper level clouds for the current climate. This is opposite to the behavior of Model II for doubled CO_2 (Hansen et al. 1984), at least for high clouds. The difference is that, while both our experiments and those of Hansen et al. imply local decreases in high clouds at the latitude of peak convection, the Model II experiments compensate with large increases in high clouds elsewhere while ours do not. All of this suggests that changes in high clouds may be sensitive to details of the parameterization of

both convective heat and moisture transports. For runs in which cumulus mass flux changes are relatively small, variations in high and middle clouds sometimes outweigh changes in low clouds to give a mean cloud top pressure variation out of phase with the shift in low cloud amount (for example, compare the control, Experiment Z, and Experiment D). Therefore, the cloud height contribution to cloud feedback may not be a simple function of convection strength.

In our experiment, downdrafts increase all types of clouds—low due to moistening of the PBL by the downdraft itself relative to pure subsidence, middle and high due to increased updraft mass and moisture flux. Thus, mean cloud height stays constant in our experiment (Table 2), suggesting that the role of downdrafts in cloud feedback will be primarily due to changes in cloud amount. The sense is that if downdrafts increase in a doubled CO₂ simulation, positive cloud feedback decreases due to the albedo effect of increased cloud cover. Current understanding of downdrafts is inadequate to predict whether they will be more or less prevalent in a warmer climate. Hookings (1965) showed that downdrafts become more vigorous with increasing cloud liquid water content. Since adiabatic liquid water content in a lifting cloud increases with temperature according to the slope of the moist adiabat (Betts and Harshvardhan 1987), it is plausible to assume that downdrafts will increase as climate warms. However, downdrafts are sensitive to other factors such as environmental relative humidity and lapse rate (Hookings 1965; Srivastava 1987), which could oppose the tendency of increased precipitation to enhance downdrafts. Even if downdraft frequency remains constant, the tendency of downdrafts to offset subsidence drying in the PBL may make low cloud cover less sensitive to changes in convection strength.

Another potential effect of downdrafts is their role in the combined feedback due to changing lapse rate and vertical distribution of water vapor. In Model II, these effects largely cancel because increased upward transport of moisture correlates with increased static stability (Hansen et al. 1984). Downdrafts, on the contrary, reduce upward moisture transport while increasing static stability (Figs. 10, 11, Table 2), so the two feedbacks cancel to a lesser extent. Once again, the sense is that increasing downdrafts are a negative feedback.

A smaller cloud feedback may actually be indicated by paleoclimate experiments done with Model II. When run with CLIMAP boundary conditions for the last ice age, the GCM gives a radiation flux imbalance of 1.6 W m^{-2} (Hansen et al. 1984). A run with ocean temperatures that are lower by 2°C gives a better simulation and is more consistent with land evidence (Rind and Peteet 1985). However, Hansen et al. note that a smaller ocean temperature discrepancy may be accommodated if cloud feedback is weaker than estimated by Model II. Weaker convection feedback may

also explain part of the discrepancy between doubled CO₂ experiments which predict large warming of the tropical upper troposphere and radiosonde observations which suggest that this region has actually cooled over the past 25 years (Angell 1986).

b. Convection–SST relationships

Attention has recently focused on observations which indicate that deep convection over the tropical oceans is limited to regions whose sea surface temperature (SST) lies above a critical value of about 27°C (Gadgil et al. 1984; Graham and Barnett 1987; Fu 1988). It has been suggested that this value of SST reflects a marginal instability criterion for atmospheric and coupled atmosphere–ocean modes driven by CISK and evaporation–wind feedbacks, SST advection, and oceanic upwelling (Lau and Shen 1988).

Figure 17 shows the longitudinal variation of cumulus heating, vertical velocity, and SST in the equatorial region (8°N–16°S) for several of our mass flux experiments. Experiment W tends to heat more and have stronger rising motion than the control over the warmest ocean waters, while the reverse is true over land. Experiment D gives a more coherent longitudinal variation of heating and lifting than the other runs over regions that are completely ocean-covered. However, to zeroth order, all the experiments exhibit the same relationship between convection, the sign of the large-scale vertical motion, and SST, regardless of how the cumulus mass flux is parameterized.

The details of the convection distribution are consistent with observations. For SST < 27°C, cumulus heating increases sharply with increasing SST. Above 27°C, convection is less sensitive to variations of SST, especially in the western Pacific, but a positive correlation between cumulus heating and SST still exists in Experiments W and D. This latter result is actually consistent with the findings of Graham and Barnett (1987) for regions of surface convergence (see their Fig. 6), although the statement is sometimes made that convection is uncorrelated with SST above 27°C.

The GCM's ability to reproduce the observations both with an arbitrary cumulus mass flux prescription and with various combinations of lifting, surface flux, and downdraft effects suggests that the convection–SST relationship is determined primarily by factors other than a fundamental unstable dynamical mode of the coupled atmosphere–ocean system. In our experiments the first layer temperature over the tropical oceans is typically 4°C lower than the SST and the temperature profile is unstable to deep convection for PBL temperatures greater than about 23°C. Thus, the change in convection regimes near the 27°C SST location in the GCM can be traced to simple thermodynamic constraints on deep convection.

Previous experiments with Model II studied the response of the Walker circulation to the removal of

continents, removal of SST gradients, and changes in mean Pacific SST (Chervin and Druyan 1984; Stone and Chervin 1984). In these experiments the suppression of convection by subsidence over the eastern Pacific was shown to be most sensitive to heating over South America and the maritime continent. In addition, when western Pacific SSTs were lowered to match those of the eastern Pacific, a significant Walker circulation remained. This suggests that the location of rising and sinking motion over the tropical Pacific is strongly constrained by continentality. Transports by this forced circulation control the moist static stability, and to a large extent this determines the location of oceanic deep convective events. SST patterns may modulate this basic circulation, but SST gradients may be more important in this regard than the magnitude of the SST itself. If there is any basis for the concept of a critical SST related to dynamical instability mechanisms, it might be tested most appropriately in a GCM by systematically varying mean SST and SST gradients with all tropical continents removed.

c. Remarks on cumulus parameterization

Although Experiment D represents a significant improvement over Model II, it has several obvious shortcomings. Equation (4), for example, relates changes in z_B to the degree of large-scale subsidence. Subsidence equals M_c without convective downdrafts, but when downdrafts are present, environmental subsidence is reduced to $M_c - M_d$, where M_d is the downdraft mass flux. Thus, M_c in (4) should also be replaced by $M_c - M_d$; the net effect would be to increase M_c , thus simulating the enhancement of convection by downdraft-initiated convergence. The crude representation of varying PBL height in (4) can be improved by including horizontal advection. A bigger problem is the inability of (4) to predict stratocumulus layers, since the height of the PBL always varies according to the LCL. One possibility is to assume that in the absence of downdrafts, convective updraft mass fluxes are limited to that required to keep PBL height constant. GATE composite easterly wave analyses, in fact, show the mixed layer height remaining roughly constant or slightly increasing during the phase in which deep cumulus updraft mass flux is a maximum (Johnson 1980, Figs. 15, 16). Undisturbed trade wind environments dominated by shallow convection also exhibit little variation in mixed layer depth (Holland and Rasmusson 1973, Fig. 3). With downdrafts, M_c could be augmented by the downdraft mass flux M_d^* from the previous convective event (cf. Frank and Cohen 1987). We would then parameterize M_c according to

$$M_c = \rho_B w_B + \frac{F_q}{\Delta q} + M_d^* \quad (5)$$

and predict the rate of change of z_B following the flow as

$$\rho_B \frac{dz_B}{dt} = \rho_B w_B + \frac{F_q}{\Delta q} - (M_c - M_d) = M_d - M_d^*. \quad (6)$$

When cumulus are present without downdrafts, (6) keeps PBL height constant. With downdrafts the PBL initially rises as the downdraft mass flux increases and is then suppressed as convection begins to diminish. When cumulus are not present, z_B may go up or down according to the net effect of large-scale motions and the surface moisture flux (for a PBL driven by dry convection). In this way thin stratocumulus layers may be predicted by comparing z_B to z_{LCL} (cf. Randall et al. 1985). We plan to conduct experiments testing this hypothesis. Alternatively, the first equality in (6) may be applied with M_c computed independently via an adjustment criterion; the effect of using such an approach for computing M_c will be discussed in a separate paper (in preparation).

It is also clear from the experiments that the contribution of surface evaporation to the cumulus mass flux is overestimated in our model, at least over the tropical oceans. Downdraft enhancement of convergence may offset this problem to some extent. Another possibility is that convergence may have a greater subgrid-scale variance than does evaporation, such that the former dominates in mesoscale areas of cloud cluster formation. The most reliable parameterization may be one which nominally predicts M_c from a modified version of (5) with the surface flux term weighted by the cluster areal extent, but which limits the convective flux to that just needed to stabilize. In this way both forcing and stability considerations can constrain convection and excessive surface flux effects may be avoided.

Our experiments demonstrate that convective downdrafts can have a noticeable positive impact on a GCM simulation. Unsaturated mesoscale downdrafts that form at the melting level are now thought to be just as important for organized convective clusters (Zipser 1977; Johnson 1980). Mesoscale updrafts associated with anvils above the melting level are less well understood but may contribute significantly to the total cluster precipitation and heating profiles (Cheng and Houze 1979; Johnson 1984). The long life cycle of mesoscale clusters, which could conceivably account for phase differences between observed diurnal cycles of convection and those simulated by our model, is not yet addressed by any moist convection scheme. Representation of these effects in future cumulus parameterizations is clearly indicated.

Much has been learned about the dynamics of tropical convection through intensive field studies such as GATE and MONEX. This paper represents one attempt to incorporate some of that knowledge into the design and validation of a cumulus parameterization scheme. Further advances in parameterization depend on a more quantitative understanding of relationships between convection and large-scale variables. In par-

ticular, the exact relationship between deep cumulus mass flux and large-scale vertical velocity, and between updraft and downdraft mass fluxes, needs to be investigated. Since these quantities are not likely to be measured with any accuracy, the best source of information may be mesoscale models. To date, such models have concentrated primarily on reproducing observed convective structures from known large-scale initial conditions. More systematic studies of the response of convection to variations of individual parameters could make mesoscale models a valuable tool for understanding convection in a broader context. Recent simulations have taken tentative steps in this direction by illustrating updraft/downdraft/wind shear relationships (Simpson et al. 1982; Weisman and Klemp 1982; Tao et al. 1987) and hold much promise for the future.

5. Conclusions

The experiments described in this paper demonstrate that the effects of both low-level convergence and surface moisture fluxes should be considered in the design of a cumulus parameterization intended for use in a global model. Downdrafts, which have not previously been incorporated in cumulus parameterizations employed in operational GCMs, have a significant impact on the simulation of tropical climate. Each of these effects should be taken into account in future assessments of cloud feedback in climate problems, because realistic modeling of convective influences appears to be central to the prediction of changes in cloud cover and vertical distribution.

A proper evaluation of the role of moist convection in determining climate sensitivity depends on the availability of adequate databases against which candidate parameterizations can be validated. Monthly global cloud retrievals about to be released by the International Satellite Cloud Climatology Project (ISCCP; Schiffer and Rossow 1985) represent an important resource for future studies of cloud/climate interactions. In addition to the primary ISCCP products relevant to radiative properties of large-scale clouds, potential information on the distribution of deep convective clouds is available. Preliminary studies with a pilot version of the data suggest that the diagnosed properties of deep convective clouds are realistic (Del Genio and Yao 1987). From the standpoint of deep convection modeling, a complementary global climatology of precipitation, which indicates vertically integrated latent heating, would be equally useful as a further constraint on parameterizations. Reliable precipitation climatologies do not exist, especially over the oceans. However, plans for a satellite mission to measure tropical rainfall are being considered (Thiele 1987). Such a dataset, combined with global cloud information from ISCCP and global analyses of the vertical profile of diabatic heating (cf. Kasahara et al. 1987), would provide a comprehensive test of the

physics of cumulus parameterization schemes used in global models.

Acknowledgments. The authors wish to thank I. Fung, J. Hansen, D. Rind, W. Rossow, P. Stone, and R. Suozzo for helpful discussions and comments during the course of this work. We are also grateful to Suozzo, R. Ruedy, and J. Lerner for their contributions to GCM code development, plotting, and production. The figures were drafted by J. Mendoza and L. del Valle. This research was supported by the NASA Climate Program.

REFERENCES

- Agee, E. M., and K. E. Dowell, 1974: Observational studies of mesoscale cellular convection. *J. Appl. Meteor.*, **13**, 46–53.
- Albrecht, B. A., 1983: A cumulus parameterization for climate studies of the tropical atmosphere. Part I: Model formulation and sensitivity tests. *J. Atmos. Sci.*, **40**, 2166–2182.
- , V. Ramanathan and B. A. Boville, 1986: The effects of cumulus moisture transports on the simulation of climate with a general circulation model. *J. Atmos. Sci.*, **43**, 2443–2462.
- Albright, M. D., E. E. Recker, R. J. Reed and R. Dang, 1985: The diurnal variation of deep convection and inferred precipitation in the central tropical Pacific during January–February 1979. *Mon. Wea. Rev.*, **113**, 1663–1680.
- Angell, J. K., 1986: Annual and seasonal global temperature changes in the troposphere and low stratosphere, 1960–85. *Mon. Wea. Rev.*, **114**, 1922–1930.
- Arakawa, A., and W. H. Schubert, 1974: Interaction of a cumulus cloud ensemble with the large-scale environment, Part I. *J. Atmos. Sci.*, **31**, 674–701.
- Baker, W. E., E. C. Kung and R. C. J. Somerville, 1977: Energetics diagnosis of the NCAR general circulation model. *Mon. Wea. Rev.*, **105**, 1384–1401.
- Betts, A. K., 1973: Non-precipitating cumulus convection and its parameterization. *Quart. J. Roy. Meteor. Soc.*, **99**, 178–196.
- , 1982: Saturation point analysis of moist convective overturning. *J. Atmos. Sci.*, **39**, 1484–1505.
- , 1986: A new convective adjustment scheme. Part I: Observational and theoretical basis. *Quart. J. Roy. Meteor. Soc.*, **112**, 677–691.
- , and Harshvardhan, 1987: Thermodynamic constraint on the cloud liquid water feedback in climate models. *J. Geophys. Res.*, **92**, 8483–8485.
- Byers, H. R., and R. R. Braham, 1949: *The Thunderstorm*. U.S. Weather Bureau, Washington, DC, 287 pp.
- Chao, W. C., 1987: On the origin of the tropical intraseasonal oscillation. *J. Atmos. Sci.*, **44**, 1940–1949.
- Cheng, C.-P., and R. A. Houze, Jr., 1979: The distribution of convective and mesoscale precipitation in GATE radar echo patterns. *Mon. Wea. Rev.*, **107**, 1370–1381.
- Chervin, R. M., and L. M. Druryan, 1984: The influence of ocean surface temperature gradient and continentality on the Walker circulation. Part I: Prescribed tropical changes. *Mon. Wea. Rev.*, **112**, 1510–1523.
- Cooper, H. J., M. Garstang and J. Simpson, 1982: The diurnal interaction between convection and peninsular-scale forcing over south Florida. *Mon. Wea. Rev.*, **110**, 486–503.
- Del Genio, A. D., and M.-S. Yao, 1987: Properties of deep convective clouds in the ISCCP Pilot Data Set. *Preprints, 17th Conf. on Hurricanes and Tropical Meteorology*, Miami, Amer. Meteor. Soc., 133–136.
- Donner, L. J., 1986: Sensitivity of the thermal balance in a general circulation model to a parameterization for cumulus convection with radiatively interactive clouds. *J. Atmos. Sci.*, **43**, 2277–2288.
- , H.-L. Kuo and E. J. Pitcher, 1982: The significance of thermodynamic forcing by cumulus convection in a general circulation model. *J. Atmos. Sci.*, **39**, 2159–2181.

- Duvel, J. P., and R. S. Kandel, 1985: Regional-scale diurnal variations of outgoing infrared radiation observed by METEOSAT. *J. Climate Appl. Meteor.*, **24**, 335–349.
- Emanuel, K. A., 1987: An air–sea interaction model of intraseasonal oscillations in the tropics. *J. Atmos. Sci.*, **44**, 2324–2340.
- Esbensen, S., 1975: An analysis of subcloud-layer heat and moisture budgets in the western Atlantic trades. *J. Atmos. Sci.*, **32**, 1921–1933.
- Frank, W. M., and C. Cohen, 1987: Simulation of tropical convective systems. Part I: A cumulus parameterization. *J. Atmos. Sci.*, **44**, 3787–3799.
- Fu, R., 1988: Properties of deep convective clouds in the tropical Pacific from analysis of ISCCP radiances. M.S. thesis, Dept. of Geological Sciences, Columbia University.
- Gadgil, S., P. V. Joseph and N. V. Jose, 1984: Ocean–atmosphere coupling over monsoon regions. *Nature*, **312**, 141–143.
- Geleyn, J. F., C. Girard and J. F. Louis, 1982: A simple parameterization of moist convection for large-scale models. *Beitr. Phys. Atmos.*, **55**, 325–333.
- Graham, N. E., and T. P. Barnett, 1987: Sea surface temperature, surface wind divergence, and convection over tropical oceans. *Science*, **238**, 657–659.
- Gray, W. M., and R. W. Jacobson, Jr., 1977: Diurnal variation of oceanic deep cumulus convection. *Mon. Wea. Rev.*, **105**, 1171–1188.
- Hansen, J., G. Russell, D. Rind, P. Stone, A. Lacis, S. Lebedeff, R. Ruedy and L. Travis, 1983: Efficient three-dimensional global models for climate studies: Models I and II. *Mon. Wea. Rev.*, **111**, 609–662.
- , A. Lacis, D. Rind, G. Russell, P. Stone, I. Fung, R. Ruedy and J. Lerner, 1984: Climate sensitivity: Analysis of feedback mechanisms. *Climate Processes and Climate Sensitivity*, J. E. Hansen and T. Takahashi, Eds., Amer. Geophys. Union, Washington, DC.
- Hartman, D. L., and E. E. Recker, 1986: Diurnal variation of outgoing longwave radiation in the tropics. *J. Climate Appl. Meteor.*, **25**, 800–812.
- , H. H. Hendon and R. A. Houze, 1984: Some implications of the mesoscale circulations in tropical cloud clusters for large-scale dynamics and climate. *J. Atmos. Sci.*, **41**, 113–121.
- Hobgood, J. S., 1986: A possible mechanism for the diurnal oscillations of tropical cyclones. *J. Atmos. Sci.*, **43**, 2901–2922.
- Holland, J. Z., and E. M. Rasmusson, 1973: Measurements of the atmospheric mass, energy, and momentum budgets over a 500-kilometer square of tropical ocean. *Mon. Wea. Rev.*, **101**, 44–55.
- Hookings, G. A., 1965: Precipitation maintained downdrafts. *J. Appl. Meteor.*, **4**, 190–195.
- Houze, R. A., Jr., and A. K. Betts, 1981: Convection in GATE. *Rev. Geophys. Space Phys.*, **19**, 541–576.
- Jaeger, L., 1976: Monatskarten des Niederschlags für die ganze Erde. *Berichte des Deutschen Wetterdienstes*, No. 139, Band 18. Offenbach a.M., 38 pp. and plates.
- Johnson, R. H., 1976: The role of convective-scale precipitation downdrafts in cumulus and synoptic-scale interactions. *J. Atmos. Sci.*, **33**, 1890–1910.
- , 1980: Diagnosis of convective and mesoscale motions during Phase III of GATE. *J. Atmos. Sci.*, **37**, 733–753.
- , 1984: Partitioning tropical heat and moisture budgets into cumulus and mesoscale components: Implications for cumulus parameterization. *Mon. Wea. Rev.*, **112**, 1590–1601.
- Julian, P. R., W. M. Washington, L. Hembree and C. Ridley, 1970: On the spectral distribution of large-scale atmospheric kinetic energy. *J. Atmos. Sci.*, **27**, 376–387.
- Kasahara, A., A. P. Mizzi and U. C. Mohanty, 1987: Comparison of global diabatic heating rates from FGGE Level IIIb analyses with satellite radiation imagery data. *Mon. Wea. Rev.*, **115**, 2904–2935.
- Knupp, K. R., and W. R. Cotton, 1985: Convective cloud downdraft structure: An interpretive survey. *Rev. Geophys.*, **23**, 183–215.
- Kuo, H. L., 1965: On formation and intensification of tropical cyclones through latent heat release by cumulus convection. *J. Atmos. Sci.*, **22**, 40–63.
- , 1974: Further studies of the parameterization of the influence of cumulus convection on large-scale flow. *J. Atmos. Sci.*, **31**, 1232–1240.
- Lau, K. M., and L. Peng, 1987: Origin of low-frequency (intraseasonal) oscillations in the tropical atmosphere. Part I: Basic theory. *J. Atmos. Sci.*, **44**, 950–972.
- , and S. Shen, 1988: On the dynamics of intraseasonal oscillations and ENSO. *J. Atmos. Sci.*, in press.
- LeMone, M. A., and W. T. Pennell, 1976: The relationship of trade wind cumulus distribution to subcloud layer fluxes and structure. *Mon. Wea. Rev.*, **104**, 524–539.
- Lindzen, R. S., 1981: Some remarks on cumulus parameterization. *Clouds in Climate: Modeling and Satellite Observational Studies*, Workshop Report, NASA Goddard Institute for Space Studies, New York, 42–51.
- , A. Y. Hou and B. F. Farrell, 1982: The role of convective model choice in calculating the climate impact of doubling CO₂. *J. Atmos. Sci.*, **39**, 1189–1205.
- McGarry, M. M., and R. J. Reed, 1978: Diurnal variations in convective activity and precipitation during Phases II and III of GATE. *Mon. Wea. Rev.*, **106**, 101–113.
- Manabe, S., and R. J. Stouffer, 1980: Sensitivity of a global climate model to an increase of CO₂ concentration in the atmosphere. *J. Geophys. Res.*, **85**, 5529–5554.
- , J. Smagorinsky and R. F. Strickler, 1965: Simulated climatology of a general circulation model with a hydrological cycle. *Mon. Wea. Rev.*, **93**, 769–798.
- Miyakoda, K., and J. Sirutis, 1977: Comparative integrations of global models with various parameterized processes of subgrid scale vertical transport: Description of the parameterization and preliminary results. *Beitr. Phys. Atmos.*, **50**, 445–487.
- Neelin, J. D., I. M. Held and K. H. Cook, 1987: Evaporation–wind feedback and low frequency variability in the tropical atmosphere. *J. Atmos. Sci.*, **44**, 2341–2348.
- Nicholls, N., and M. A. LeMone, 1980: The fair weather boundary layer in GATE: The relationship of subcloud fluxes and structure to the distribution and enhancement of cumulus clouds. *J. Atmos. Sci.*, **37**, 2051–2067.
- Nitta, T., 1978: A diagnostic study of interaction of cumulus updrafts and downdrafts with large-scale motions in GATE. *J. Meteor. Soc. Japan*, **56**, 232–241.
- Ogura, Y., Y.-L. Chen, J. Russell and S.-T. Soong, 1979: On the formation of organized convective systems observed over the GATE A/B array. *Mon. Wea. Rev.*, **107**, 426–441.
- Oort, A. H., 1983: Global atmospheric circulation statistics, 1958–1973. NOAA Prof. Pap. 14, U.S. Dept. of Commerce, Washington, DC, 180 pp. and 47 microfiches.
- Prather, M., M. McElroy, S. Wofsy, G. Russell and D. Rind, 1987: Chemistry of the global troposphere: Fluorocarbons as tracers of air motion. *J. Geophys. Res.*, **92**, 6579–6613.
- Randall, D. A., J. A. Abeles and T. G. Corsetti, 1985: Seasonal simulations of the planetary boundary layer and boundary-layer stratocumulus clouds with a general circulation model. *J. Atmos. Sci.*, **42**, 641–676.
- Reed, R. J., and E. E. Recker, 1971: Structure and properties of synoptic scale wave disturbances in the equatorial western Pacific. *J. Atmos. Sci.*, **28**, 1117–1133.
- Rind, D., 1986: The dynamics of warm and cold climates. *J. Atmos. Sci.*, **43**, 3–24.
- , and W. B. Rossow, 1984: The effects of physical processes on the Hadley circulation. *J. Atmos. Sci.*, **41**, 479–507.
- , and D. Peteet, 1985: Terrestrial conditions at the last glacial maximum and CLIMAP sea-surface temperature estimates: Are they consistent? *Quaternary Res.*, **24**, 1–22.
- Roeckner, E., U. Schlese, J. Biercamp and P. Loewe, 1987: Cloud optical depth feedbacks and climate modelling. *Nature*, **329**, 138–140.
- Saltzman, B., 1970: Large-scale atmospheric energetics in the wavenumber domain. *Rev. Geophys. Space Phys.*, **8**, 289–302.

- Schiffer, R. A., and W. B. Rossow, 1985: ISCCP global radiance data set: A new resource for climate research. *Bull. Amer. Meteor. Soc.*, **66**, 1498–1505.
- Simpson, J., G. Van Helvoirt and M. McCumber, 1982: Three-dimensional simulations of cumulus congestus clouds on GATE day 261. *J. Atmos. Sci.*, **39**, 126–145.
- Smagorinsky, J., 1982: Carbon dioxide and climate: A second assessment. National Academy of Sciences, National Research Council, Washington, DC.
- Somerville, R. C. J., and L. A. Remer, 1984: Cloud optical thickness feedbacks in the CO₂ climate problem. *J. Geophys. Res.*, **89**, 9668–9672.
- Srivastava, R. C., 1987: A model of intense downdrafts driven by the melting and evaporation of precipitation. *J. Atmos. Sci.*, **44**, 1752–1773.
- Stone, P. H., and R. M. Chervin, 1984: The influence of ocean surface temperature gradient and continentality on the Walker circulation. Part II: Prescribed global changes. *Mon. Wea. Rev.*, **112**, 1524–1534.
- , and G. Salustri, 1984: Generalization of the quasi-geostrophic Eliassen–Palm flux to include eddy forcing of condensation heating. *J. Atmos. Sci.*, **41**, 3527–3536.
- Tao, W.-K., J. Simpson and S.-T. Soong, 1987: Statistical properties of a cloud ensemble: A numerical study. *J. Atmos. Sci.*, **44**, 3175–3187.
- Thiele, O. W., Ed., 1987: *On Requirements for a Satellite Mission to Measure Tropical Rainfall*. NASA RP-1183, National Aeronautics and Space Administration, Washington, DC, 49 pp.
- Thompson, R. M., Jr., S. W. Payne, E. E. Recker and R. J. Reed, 1979: Structure and properties of synoptic-scale wave disturbances in the intertropical convergence zone of the eastern Atlantic. *J. Atmos. Sci.*, **36**, 53–72.
- Tiedtke, M., 1984: The effect of penetrative cumulus convection on the large-scale flow in a general circulation model. *Beitr. Phys. Atmos.*, **57**, 216–239.
- Wang, W.-C., W. B. Rossow, M.-S. Yao and M. Wolfson, 1981: Climate sensitivity of a one-dimensional radiative-convective model with cloud feedback. *J. Atmos. Sci.*, **38**, 1167–1178.
- Washington, W. M., and G. A. Meehl, 1984: Seasonal cycle experiment on the climate sensitivity due to a doubling of CO₂ with an atmospheric general circulation model coupled to a simple mixed-layer ocean model. *J. Geophys. Res.*, **89**, 9475–9503.
- Weisman, M. L., and J. B. Klemp, 1982: The dependence of numerically simulated convective storms on vertical wind shear and buoyancy. *Mon. Wea. Rev.*, **110**, 504–520.
- Wetherald, R. T., and S. Manabe, 1986: An investigation of cloud cover change in response to thermal forcing. *Clim. Change*, **8**, 5–23.
- Wilson, C. A., and J. F. B. Mitchell, 1987: A doubled CO₂ climate sensitivity experiment with a global climate model including a simple ocean. *J. Geophys. Res.*, **92**, 13 315–13 343.
- Yao, M.-S., and P. H. Stone, 1987: Development of a two-dimensional zonally averaged statistical-dynamical model. Part I: The parameterization of moist convection and its role in the general circulation. *J. Atmos. Sci.*, **44**, 65–82.
- Zipser, E. J., 1977: Mesoscale and convective-scale downdrafts as distinct components of squall-line circulation. *Mon. Wea. Rev.*, **105**, 1568–1589.